June 2021

Characterization and Optimization of the Electrochemical Phosphate Sensor

Rakesh Sen
University of Wisconsin-Milwaukee

CHARACTERIZATION AND OPTIMIZATION OF ELECTROCHEMICAL PHOSPHATE SENSOR

by

Rakesh Sen

A Thesis Submitted in

Partial Fulfillment of the

Requirements for the Degree of

Master of Science

in Engineering

at

The University of Wisconsin-Milwaukee

August 2021

ABSTRACT

CHARACTERIZATION AND OPTIMIZATION OF THE ELECTROCHEMICAL PHOSPHATE SENSOR

by

Rakesh Sen

The University of Wisconsin-Milwaukee, 2021
Under the Supervision of Dr. Woo-Jin Chang

This research implies on making a noble low cost-effective electrochemical sensor based on fabrication of AM (Ammonium Molybdate) and Py (Pyrrole) nanocomposite to detect phosphate in water. The developed sensor was tested with various concentrations of phosphate solutions in a wide range of pH (pH 6-pH 7.5) to determine the sensitivity and lower detection limit. With a lowest detection limit of 10^{-11} mol/L, an Ammonium Molybdate and Pyrrole (AM-Py as layer) nanocomposite modified screen printed electrode (SPE) produced the best signal using open circuit voltammetry (OCV) method. To observe the pH effect on the proposed sensor, it was tested with the phosphate buffer solutions (range from pH 6-pH 7.5). The signals from open circuit voltammetry were analyzed, and the related parameters were optimized. In comparison to the complex and time-consuming electrochemical synthesis process, the established sensor's structure and fabrication method are quick and easy to follow. Furthermore, for low-cost mass manufacturing, this fabrication process can be easily changed and implemented using a printing unit. The developed electrochemical sensor, according to the findings, has the ability to detect phosphate anion with a high precision rate.

This is dedicated to
my family and friends

TABLE OF CONTENTS

LIST OF FIGURES

LIST OF TABLES

LIST OF ABBREVIATIONS

LOD	Limit of Detection
CV	Cyclic Voltammetry
OCV	Open circuit voltammetry
OCPT	Open Circuit Potential-Time
Py	Pyrrole
AM	Ammonium Molybdate
SPE	Screen Printed Electrode
GCE	Glassy Carbon Electrode
DI	Deionized Water
SEM	Scanning Electron Microscope
EDS	Energy Dispersive Spectroscopy
IUPAC	International Union of Pure and Applied Chemistry
WHO	World Health Organization
EPA	United States Environmental Protection Agency

ACKNOWLEDGEMENTS

First, I would like to express my gratitude to my advisor Prof. Dr. Woo Jin Chang for accepting me into his research group and also express my heartfelt thanks to him for his guidance, encouragement and continuous support during my graduate studies and research. His enthusiasm for teaching and research offered challenging opportunities to expand my scientific knowledge and growing interest in the Electrochemical Sensor field. I am also grateful to my lab mate Mohammad Rizwen Ur Rahman for providing me the assistance needed to learn the fabrication process of nanocomposites.

Dr. Steven Hardcastle (Manager, Advanced Analysis Facility) provided me with excellent scanning electron microscope (SEM) training, which aided me in investigating the surface of the nanocomposites.

Dr. Yongjin Sung and Dr. Ben Church were also members of my thesis committee, which I am grateful for. I appreciate their taking the time to review my work. I am grateful to my family for their love, support, and well wishes, which have enabled me to complete my study without their presence. I am also indebted to my close friends for being the inspiration behind my working force.

Chapter 1: Introduction

1.1 Structure of Thesis

This study aims to investigate the electrochemical identification of phosphate ions in water. One of the electroanalytical techniques used in this study was open circuit voltammetry (OCV) for phosphate ion trace analysis. The electrochemical sensor's fabrication process and working theory are explored in depth. A comparison of different phosphate solution concentrations, as well as the effects of various operating conditions, is also illustrated. A brief background based on a similar electrochemical sensor structure for detecting phosphate ions is presented in Chapter 1. This chapter covers material selection for target analytes as well as electrochemical sensor fabrication techniques. The methods of manufacture, the materials and devices used in this study is discussed in Chapter 2. Chapter 3 contains the electrical sensor working mechanism for the detection of phosphate ions. It discusses the proposed nanocomposite structure and how to make the precursor solutions prior to test. Most importantly, morphological surface study of the working electrode is also investigated in this chapter. The comparison of optimum operating conditions with respect to physical parameters, the measurement of different phosphate concentration, and buffer solution test are all covered in Chapter 4. The importance of pH in the electrochemical detection of phosphate ions is one of the most important section in Chapter 4. This chapter also provides a comparative analysis of optimal operating conditions. The conclusion of Chapter 5 includes the overall application, drawbacks, and a description of the developed sensor. The proposed electrochemical sensor's future path and application are also addressed at the end of this chapter.

1.2 Motivation/Literature Review

Phosphate (PO_4^{-3}) is a nonmetallic essential plant nutrient and chemical compound that is needed for plant and animal development. Many fertilizers contain calcium hydrogen phosphate ($CaH_4P_2O_8$) which is commonly referred to as "Superphosphate" [1]. Phosphorus is the eleventh most abundant mineral in the earth's crust, and it's involved in the formation of deoxyribonucleic acid (DNA), ribonucleic acid (RNA), adenosine diphosphate (ADP), and adenosine triphosphate (ATP) (ATP). Too much nitrogen and phosphorus, on the other hand, pollute the air and water [1], typically as a result of a broad variety of human activities. Eutrophication (excessive aquatic plant growth) in lakes, rivers, and streams is often caused by too much nitrogen and soluble reactive phosphate (i.e. phosphorus) in the water. Algal growth degrades water quality, depletes food resources, and harms fish and other marine life ecosystems. Most notably, eutrophication decreases or removes oxygen in the water, causing illnesses in fish and mass mortality [2]. For past numerous decades, nutrient contamination has wreaked havoc on many streams, rivers, lakes, bays, and coastal waters, causing major environmental, human health and economic problems [2]. Algae blooms may involve blue-green algae (cyanobacteria), which release toxins into the water, as was the case in Lake Erie, USA, in the summer of 2014 [2], [3]. For many days, the water from the Toledo water treatment plant was undrinkable.

Phosphate is not harmful in itself, and the health effects of phosphates in drinking water are unknown [5–7]. The Food and Drug Administration (FDA) reported in a study on the toxicology of inorganic phosphates as food additives that phosphates are commonly accepted as safe as a food additive. Maximum phosphate product dosages in drinking water, as well as other water treatment additives, are maintained by NSF International [8]. The average phosphate levels in a liter of

drinking water (0.025 mg/L) are around a hundred times higher than the phosphate levels in a normal American diet. For example, the amount of phosphates in one can of soda is equivalent to about twelve liters of water within the recommended allowance of phosphates in water [7]-[9].

Phosphates are widely applied to drinking water as a corrosion/rust inhibitor by public water systems (PWSs) to resist lead and copper leaching from metal pipes and fixtures [5-6]. When inorganic phosphates (such as phosphoric acid, zinc phosphate, and sodium phosphate) are applied to water, they form orthophosphate, which generates an insoluble mineral layer on the inside of pipes, sewers, and household plumbing. The coating prohibits breaking down of corrosion elements from metal complexes on the metal pipes. Based on the supply water quality, the PWSs maintain the appropriate orthophosphate levels (around 300 ppb) to minimize corrosion [5].

Inorganic and/or organic phosphorus may form phosphate in water due to its nature and may be available in the particulate phase or in the dissolved phase. Living and dead plankton, phosphorus precipitates, phosphorus adsorbed to particulates, and amorphous phosphorus are all examples of particulate matter. Inorganic phosphorus (usually in the soluble orthophosphate form), organic phosphorus excreted by animals, and macromolecular colloidal phosphorus make up the dissolved process. Phosphorus is continually converted into particulate and soluble organic and inorganic forms. Dissolved phosphorus (usually as orthophosphate) is assimilated to phytoplankton and modified to organic phosphorus. There are many contributors of phosphate, both natural and human. Phosphates enter water by drainage from phosphate-containing fertilizer-treated agricultural areas, lawns and golf courses, livestock and poultry-feeding operations, pet wastes, food-processing wastes, pulp, and paper industry wastewater, and partially treated or untreated sewage [5],[10]. Several biological reactions in the atmosphere ultimately transform all phosphorus to inorganic forms [5]. H_3PO_4 (phosphoric acid), $H_2PO_4^-$ (dihydrogen phosphate),

$H_2PO_4^{2-}$ (hydrogen phosphate), and PO_4^{3-} (orthophosphate) are the four states of soluble phosphorus in natural water [11]. The Environmental Protection Agency (EPA) and the Department of Natural Resources (DNR) both developed strict guidelines for effluent water streams from factories to rivers, reservoirs, and watersheds [12]– [14]. An algal bloom could be triggered by a soluble reactive phosphate concentration of about 0.05 mg/L [5]. Another challenge in drinking water quality is dissolved phosphate [15]. In water treatment plants, phosphorus levels greater than 1.0 ppm (mg/L) can create interference with coagulation [15]. Phosphate concentration control is therefore critical for preserving water quality and reducing nutrient contamination [2], [5], [11], [16]. Continuous and on-site monitoring is necessary to effectively regulate industrial effluent and drinking water, which necessitates the development of a low-cost, responsive, small-size phosphate sensor. Method 300.1 ion chromatography is the standard analytical method permitted and recommended by the US EPA for determining phosphate and a set of other inorganic anions in reagent water, surface water, ground water, and drinking water [17]. Precipitation as a type of magnesium pyrophosphate ($Mg_2P_2O_7$ or $Mg_2O_7P_2$) and magnesium ammonium phosphate hexahydrate ($NH_4MgPO.6H_2O$), titration with sodium hydroxide, and chromatography are some of the most popular analytical methods for routine phosphate determination [18]– [24]. However, these methods involve sample pre-treatment, are time and reagent intensive, and often have low selectivity. Colorimetry after dissolution [25]– [29], ion chromatography [29]– [32], flow injection analysis [33], [34], and potentiometry [35], [36] are all examples of instrumental methods that are used to evaluate samples. The traditional instrumental methods are sensitive, with detection limits ranging from 20 to 150 nmol/L. Traditional methods for detecting phosphate in aqueous media require highly trained personnel and are not appropriate for in-situ measurements.

Previous studies have identified biosensors for glucose [37], DNA [38], urea [39], phosphate [40], and other compounds. Non-experts may use a phosphate biosensor by following basic step-by-step instructions, and the unit is inexpensive and portable for on-site research. The two types of biosensors are enzyme biosensors and screen-printed electrode (SPE) sensors. Enzyme biosensors are easy to make and do not need any pre-treatment or reagents [34]. The SPE sensor is suitable for electrochemical detection methods that require less time to measure, provide precise phosphate measurements, and have a high selectivity. However, most of these methods do not allow for direct or field phosphate calculation and require the use of heavy metal ions and hazardous chemicals, all of which may be harmful to human health and the environment. Biosensors that use an electrochemical detection method usually have higher sensitivity and selectivity, as well as a lower detection limit. Amperometric detection using four enzyme systems, such as MP, MR, GODx, and AP, for example, has the lowest detection limit of the methods mentioned, which is 0.01 mmol/L. The detection method that uses several enzymes, on the other hand, has a limited linear range and low reproducibility depending on the operating conditions. Over the last few decades, screen-printed electrodes (SPE) have been used as low-cost electrochemical detection methods. SPEs are now used as cost-effective electrochemical substrates due to substantial improvements in both their format and printing materials over the last decade. Because of their beneficial material properties, such as disposability, simplicity, and rapid responses, SPEs have been successfully used for rapid in site analysis of environmental contaminants [40]– [45].

Table 1 Lower detection limit and used materials of reported detection methods to determine inorganic and organic phosphate [41]

Sensing Method	**Materials used**	**LOD (µmol/L)**
ISE	Molybdate complex	0.6
Ion chromatography	Molybdate complex	0.1
Amperometry	Molybdate complex	3
Amperometry	NPN, XOD, AP	2
Amperometric	Poly (carbamoylsulphonate) (PCS) hydrogel immobilized pyruvate oxidase	50
Amperometric	Immobilized Maltose phosphorylase, acid phosphatase, glucose oxidase and mutarotase on a regenerated cellulose	0.01
Fluorescent probe	PVC matrix	5
Florescent PVC matrix	NP, XOD, HRP Almorine	3
Potentiometric	NPN/XOD	20
Fluorescent	Molybdate and thamine	NA
Amperometric	MP, MR, GODx, AP	0.01
Capacitance	Malachite green	0.2
Amperometric	Immobilization of pyruvate oxidase (PyOx) on a polyioncomplex membrane	0.2
Conductometry	AP/BSA/GLA	0.4
Plant tissue electrode	Inhibition by phosphate of potato acid phosphatase catalyzed glucose and phosphate	25
Screen-printed electrode	Immobilizing pyruvate oxidase (PyOD)	3.6

A few portable phosphate detectors with prices ranging from $50 to $500 have recently been developed (Hanna Instruments, Thermo Fisher Scientific, Lamotte Instruments, and Milwaukee Instruments) [46]. Optical methods are used in these detectors, with detection limits ranging from 20 to 150 nmol/L [47]-[49]. Fluorescence, luminescence, chemiluminescence, and spectrophotometric detection are examples of optical detection methods. Optical approaches, on the other hand, are often hampered by the interference, are inconsistent, and have minimal selectivity [50]– [52]. Table 1 summarizes the lower detection limit of traditional methods for detecting inorganic and organic phosphate. As mentioned in Table 1, biosensors, electrochemical sensors, ion sensitive electrodes (ISE), and screen-printed electrodes have all been used to develop methods other than optical methods (SPE).

Phosphate (PO_4^{3-}) is an inorganic chemical and a phosphoric acid based on salt-forming anion. Phosphate is a polyatomic ion with the empirical formula (PO_4^{3-}) and a molar mass of 94.97 g/mol and a molar mass of 94.97 g/mol. There are four types of aqueous phosphate. The phosphate ion (PO_4^{3-}) predominates in strongly basic conditions, while the hydrogen phosphate ion (HPO_4^{2-}) predominates in weakly basic conditions. The dihydrogen phosphate ion ($H_2PO_4^-$) is the most common ion in weakly acidic conditions. The dominant form in highly acidic conditions is tri-hydrogen phosphate (H_3PO_4) .Specifically, consider the following three equilibrium reactions:

$$H_3PO_4 \rightleftharpoons H^+ + H_2PO_4^-; \qquad H_2PO_4^- \rightleftharpoons H^+ + HPO_4^{2-}; \qquad HPO_4^{2-} \rightleftharpoons H^+ + PO_4^{3-}$$

As phosphoric acid is dissolved in water, it ionizes, as seen in the (aqueous solution) below. The anion of $H_2PO_4^-$(dihydrogen phosphate anion) is formed when H_3PO_4(phosphoric acid) dissociat es, and the value of pH is 4.5. Potassium dihydrogen phosphate (KH_2PO_4), Dipotassium phosphate (K_2HPO_4), Sodium dihydrogen phosphate (NaH_2PO_4), and Disodium phosphate (Na_2-HPO_4) were used to get the phosphate anions.

The phosphate anion's balanced equation and ionic reaction are as follows:

$$KH_2PO_4 + H_2O \rightarrow KOH + H_3PO_4$$

$$K_2HPO_4 + 2H_2O \rightarrow 2KOH + H_3PO_4$$

$$NaH_2PO_4 + H_2O \rightarrow NaOH + H_3PO_4$$

$$Na_2HPO_4 + H_2O \rightarrow 2NaOH + H_3PO_4$$

All the above reaction's have H_3PO_4 as their byproduct. Phosphate anion is obtained from this.

$$H_3PO_4 + H_2O \rightleftharpoons H_3O^+ + H_2PO_4^-$$

Total ionic equation will be: $K^+ + H_2PO_4^- + H_2O \rightarrow K^+ + OH^- + 3H^+ + PO_4^{3-}$

The net ionic equation: $H_2PO_4^- + H_2O \rightleftharpoons +OH^- + 3H^+ + PO_4^{3-}$

AM has been used for colorimetric identification and analytical analysis of phosphate in water [58], [59], [64]. AM is involved in the formation of molybdophosphoric acid, which is then reduced to the highly colored complex molybdenum blue [26]. The potential of the system changes when molybdophosphoric acid [MPA.$H_3PMo_{12}O_{40}$] is formed. This can be used as a selective detection device for phosphate ions in water [65] by combining AM with a screen-printed electrode.

$H_3PO_4 + 6Mo(VI)_t \leftrightarrow$ 12-MPA + $9H^+$

AM [$(NH_4)_6MO_7O_{24}.4H_2O$] produces a molybodate phosphate complex in strong acidic media. This complex can be reduced to a mixed molybdenum oxidation state and amperometry can be used to detect it at low potential [66].

$7H_3PO_4 + 12Mo_7O_{24}^{6-} + 51H^+ \rightarrow 7PMo_{12}O_{40}^{3-} + 36H_2O$

$PMo_{12}O_{40}^{3-} + 2e^- \rightarrow PMo_{10}^{6+}Mo_2^{5+}O_{40}^{3-}$

Carbon was tested with Ammonium Molybdate and Pyrrole due to its high conductivity. Wide surface area, fast electron transfer rate, increased mass transport rate, enhanced electro catalytic properties, lower solution resistance, and higher signal-to-noise ratio are all advantages of the Ammonium Molybdate and Pyrrole nanocomposite.

AM was used to create a phosphate sensor in this research. PY was used with the compound as layers or as a mixture of the interference of potassium chloride (for presence of Cl) on phosphate sensing were characterized using established low-cost electrochemical phosphate sensor for better sensitivity and selectivity.

1.3 Open Circuit Potential Method

Electroanalytical methods based on electrochemical principles are commonly used for tracking industrial materials, scientific research, and environmental analysis due to their advantages over traditional analytical techniques. Among them, Open Circuit Potential (OCP) is one of the most conventional and popular technique. It is also known as open circuit voltage, zero-current potential, corrosion potential, equilibrium potential, or rest potential [67].

1.3.1 Overview of Technique

The Open Circuit Potential (OCP) experiment is a passive application. The potentiostat's counter electrode circuitry (which is needed to transfer current through the cell) is bypassed by passive. Only the resting potential between the reference and working electrodes is calculated in this mode. This is not to suggest that the chemical system is in full equilibrium. In fact, some

systems might be out of control, with their passive potential shifting because of homogeneous reactions. OCP is exceptional in that it is a thermodynamically mainly electrolytic method.

Researchers may be concerned about the stability of their electrochemical system. One approach that helps to answer this question is OCP. A constant OCP (generally ±5 mV or less) over long periods of time (minutes) shows that the program is thermodynamically stable, or at least stable enough for a perturbation-based experiment. The analytical certainty of a measurement based on a flat baseline is far larger than that of a sloping baseline, particularly if the inclined baseline is not well specified, modeled, or constant.

Despite the fact that calculating OCP is a relatively simple task for a potentiostat, it can still be a useful experiment. The OCP is simply the potential difference between the working and reference electrodes since i=0, either by disconnecting the counter electrode or by inserting a very high impedance resistor in its direction to prevent current passage.

$$\mathrm{E_{OCP}} = E_{Working} - E_{Reference}$$

As a result, a potentiostat can be used to calculate the potential difference between two points like a basic voltmeter.

1.3.2 Principal Equation

Considering the general electrochemical reaction,

$$O + ne^- \leftrightharpoons R$$

In a n electron transfer reaction, O is reduced to R, with formal (thermodynamic) potential E^0. Using the Nernst Equation, the ratio of O and R can be calculated by measuring the OCP.

$$E = E_0 + \frac{RT}{nF} \ln \left(\frac{C_0}{C_R}\right)$$

where R is the Universal Gas Constant (8.314 J/mol K), T is absolute temperature, n is the number of electrons, and F is Faraday's Constant (96,485 C/mol). When OCP is identified, the Nernst equation can be used to determine the species concentration ratio.

Multiple working electrodes systems can be considered for multiplex detection using the electrochemical process. Interference between working electrodes becomes a major issue in such a device. One way to solve this problem is to simply repeat the voltammetry for each working electrode one by one, but this takes a long time. Another disadvantage is that the amperometric and voltammetric approaches require a complicated voltage supply source to apply and scan the potential. Open circuit potential (OCP) appears to be an appealing detection method for the design of simple biosensors in this regard [68,69,70].

OCP uses neither potential nor current to calculate the differences in potential between working electrodes immersed in medium solution and a suitable reference electrode. The OCP technique has many advantages over voltammetry and amperometry, including a two-electrode mode with working and reference electrodes, spontaneous calculation of the electrode potential built by electrochemical reactions on the electrode surface, the ability to miniaturize the reference electrode, and the ability to acquire several electrode potentials at once.

Furthermore, since OCP tests all redox reactions without applying any voltage, there is less contamination [71]. Therefore, OCP can be used to simplify and miniaturize electrochemical systems for use in labs or in the field for clinical diagnosis.

Chapter 2: Theory and Application

2.1 Chemicals, Materials and Reagents

Potassium dihydrogen phosphate (KH_2PO_4), Dipotassium phosphate (K_2HPO_4), Sodium dihydrogen phosphate (NaH_2PO_4), and Disodium phosphate (Na_2HPO_4), all purchased from EMD Millipore, were used to make standard phosphate solutions with various concentrations. Different buffers solutions were made using those chemicals. All the other chemicals and reagents used in this experiment were analytical grade from Sigma-Aldrich, including Acetone (ACS reagent, ≥ 99.5%), PY (reagent grade, 98%), NaCl, Sulfuric acid, and AM Tetrahydrate (Bioreagent, 81.0-83.0% M_0O_3 basis). All the solutions were made with deionized water, supplied from EMS (Engineering & Mathematical Sciences Bldg.), University of Wisconsin Milwaukee.

2.2 Devices, Instruments and Measurements

2.2.1 Screen Printed Electrodes (SPE)

Screen-printed electrodes (SPEs) are a good alternative to glassy carbon electrodes (GCEs), traditional cumbersome electrodes and cells, and the use of electrochemical methods with less oxygen intrusion. With major advancements in both format and printing materials over the last decade, are now used as cost-effective electrochemical substrates [74]. Because of their beneficial material properties, such as disposability, simplicity, and rapid responses, SPEs have been successfully used for rapid in site analysis of environmental contaminants [26, 30, 57, 72, 73]. Because of the SPEs' easy handling and control in a disposable manner, problems associated with oxidation or biofouling can now be avoided, as well as the risk of damage associated with a costly reusable sensor. A three-electrode Screen Printed Electrode (SPE) sensor-based graphite powder was used in this analysis, as shown in Figure 1. Nanostructured technology for screen-printed thick

film electrochemical sensors makes them accessible and long-lasting for electrochemical analysis in environmental, clinical, or agri-food settings.

A traditional screen-printed three-electrode device (from eDAQ Pty Ltd.) was used, with graphitic carbon powder as the working electrode (3 mm diameter disk), graphitic carbon powder as the counter electrode (outer annular crescent), and Ag/AgCl pellet as the reference electrode.

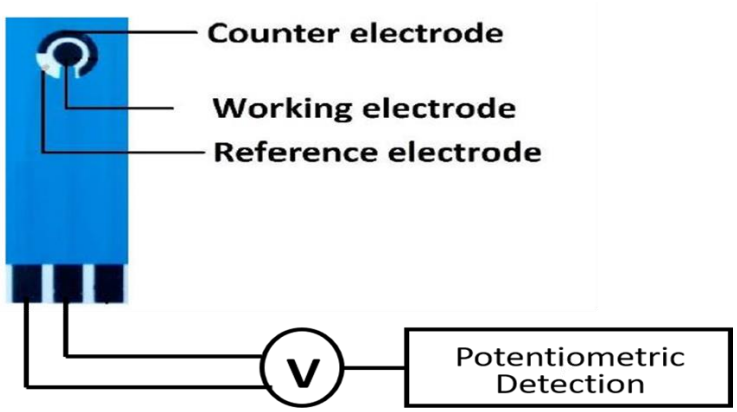

Figure 1 : A three-electrode Screen Printed Electrode (SPE) sensor (50 x 13 mm / h x w)

2.2.2 Electrochemical Analyzer (CHI-6012E)

The CHI-6012E (Figure 2) computer-controlled electrochemical analyzer was used for all electrochemical measurements (CHI, USA). The Model 600E series is intended for electrochemical measurements in general. A fast digital function generator, a direct digital synthesizer for high frequency AC waveforms, high-speed dual-channel data acquisition circuitry, a potentiostat, and a galvanostat are all included in the system. The actual control range is ±250 mA and the future control range is ±10 V. The instrument can measure currents as low as picoamperes. The function generator has a 10 MHz update rate. Both current and potential (or an external voltage signal) can be sampled concurrently at a rate of 1 MHz with 16-bit resolution

using two high-speed and high-resolution data acquisition channels. The instrument's dynamic range of experimental time scales is broad. In cyclic voltammetry, for example, the scan rate may be as high as 1000 V/s with a 0.1 mV potential increment or 5000 V/s with a 1 mV potential

Figure 2: CHI-6012E, a computer-controlled electrochemical analyzer (CHI, USA)

increment. The potentiostat / galvanostat has four electrodes, allowing it to be used for liquid/liquid interface calculations and removing the effect of connector and relay contact resistance for high current measurements. During an electrochemical measurement, the data acquisition systems often enable an external input signal (such as spectroscopic) to be collected continuously [75].

2.2.3 The Scanning Electron Microscope & Energy Dispersive Spectroscopy (EDS)

(SEM) images were taken in the Advanced Analysis Facility (AAF) at the College of Engineering & Applied Science, University of Wisconsin-Milwaukee, using the JEOL JSM-6460 LV with Energy Dispersive Spectroscopy and the Plasma Sputter Coating equipment.

A scanning electron microscope (SEM) uses a directed beam of high-energy electrons, allowing for much higher magnification, resolving power, and depth of field than an optical microscope. The surface morphology and elemental composition of a sample can be determined using SEM. Depending on the type of specimen and required resolution, specimens may be observed in high or low vacuum. In order to achieve high resolution images, some non-conductive samples must be sputter coated with a very thin layer of gold (20nm).

SEM can also determine the elemental composition of selected areas within a sample when used in conjunction with Energy Dispersive Spectroscopy (EDS). Relevant elements and their chemical compositions within a sample can be defined using EDS. Its X-ray spectral characterization capabilities are based on the fundamental concept that each element has a unique atomic structure that produces a distinct set of peaks.

The JEOL JSM 6460LV scanning electron microscope is well-resourced for submicron imaging in biology, materials science, microelectronics, and some nanotechnology applications. It can analyze and classify particles, fracture and failure analysis, surface morphologies, composite materials, and microstructures of prepared cross sections [76].

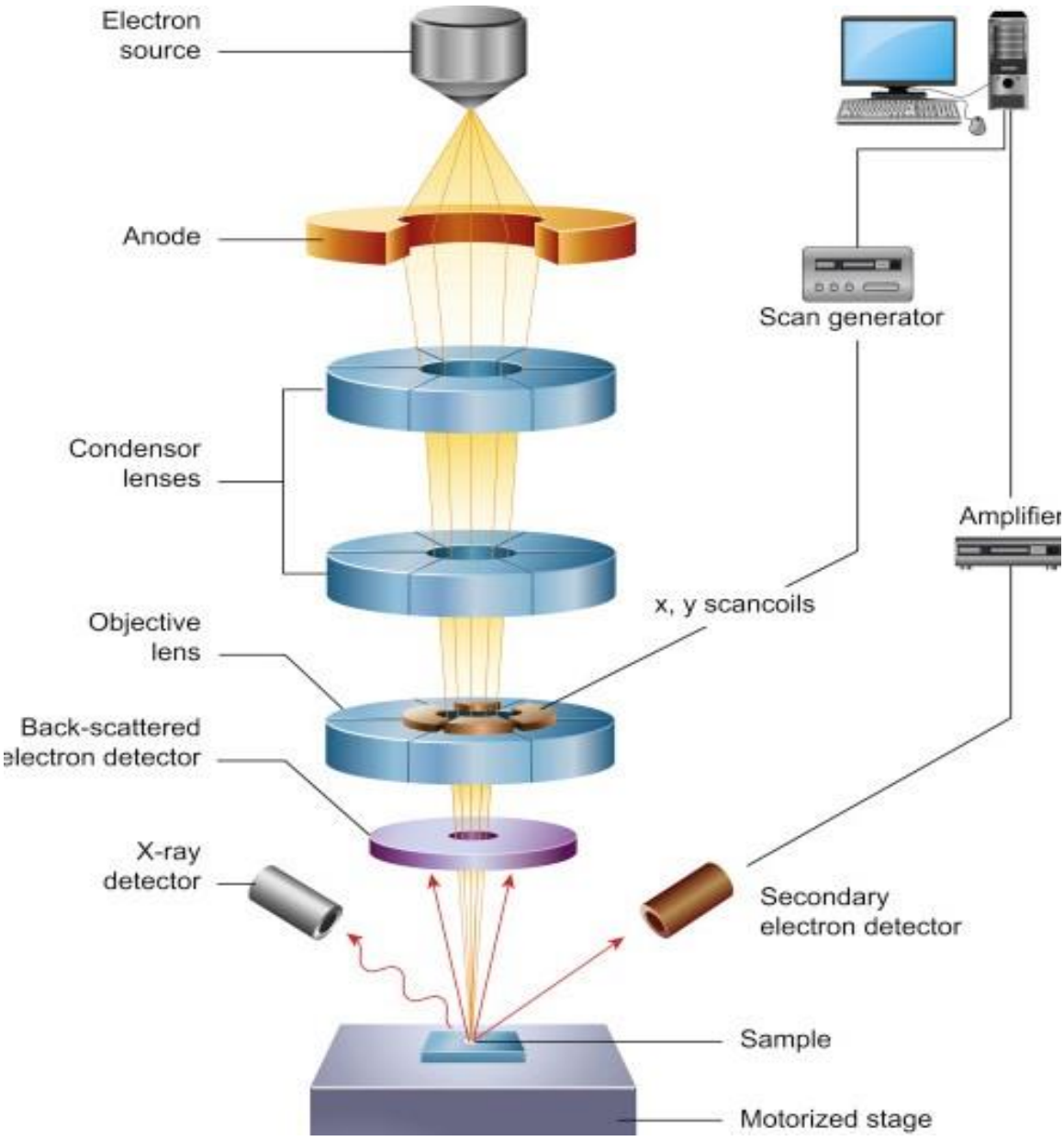

Figure 3: Schematic diagram of the core components of an SEM microscope [77]

2.3 Properties of Nanocomposite Materials

Different combination of nanocomposites was tested to detect phosphate in aqueous solution. But in terms of broad surface area, increased mass transport rate, improved electro-

catalytic properties, lower solution resistance, and higher signal-to-noise ratio, the combination of Pyrrole and Ammonium Molybdate nanocomposite has shown the best result with high sensitivity. Due to their stable chemical properties, they were chosen over other materials.

2.3.1 Chemical Properties of Pyrrole (C_4H_5N)

Pyrrole is a five-membered heterocyclic compound of one nitrogen atom that is colorless at room temperature, occurs naturally in coal tar and bone oil, turns black in the air rapidly, and has a strong irritant odor. The boiling point is 130°C, the freezing point is -24°C, and the relative density is 0.9691. It is insoluble in water and dilute alkali solutions, but it is soluble in alcohol, ether, benzene, and mineral acid solutions. When exposed to light or air, it quickly polymerizes into dark red resin trimer in the presence of a small amount of inorganic acid. When processed, it's chemical properties can spoil if exposed to light or air. Five sp2 hybrid atoms on the pyrrole ring are in the same plane, one pair of non-shared electrons of the nitrogen atom occupy the p-orbital, four carbon atoms and the p-orbital are parallel and overlapping, creating 5 atoms, 6 electrons closed conjugated framework with aromatic character and susceptibility to electrophilic substitution reactions. As a result, the alkalinity of the nitrogen atom in pyrrole is low (pKb13.6); on the other hand, the hydrogen on the nitrogen atom produces a weak acid.

Pyrrole is the basic structural unit of heme, chlorophyll, bile pigments, a few amino acids, a few alkaloids, and a few enzymes; these compounds have powerful physiological activity and drug-like properties. The hydrogenated pyrrole ring structure can be found in vitamin B12, glycopyrrolate, kainic acid (roundworm medicine), and clindamycin (antibiotic) medicines. Since 1979, it has been discovered that electrochemical oxidation of pyrrole can produce a flexible conductive polymer film with a conductivity of 104 S/m and good stability.

With several usage like assessing the concentration of gold selenite and silicic acid, Pyrrole can be used to determine chromate, gold, iodine salt, mercury, selenious acid, silicon, and vanadium [78].

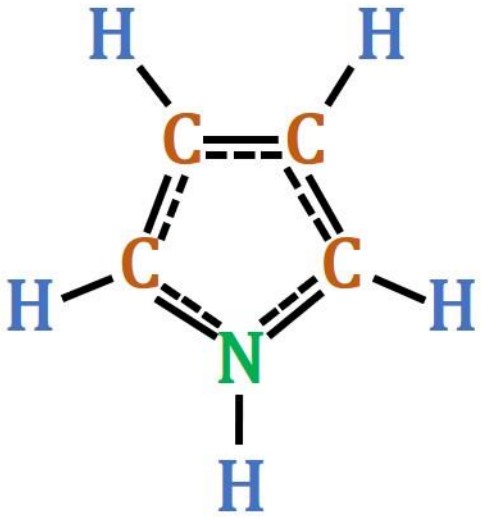

Figure 4: Atomic structure of Pyrrole (C_4H_5N)

2.3.2 Chemical Properties of Ammonium Molybdate {$(NH_4)_6Mo_7O_{24}$}

The ammonium molybdate tetrahydrate (also known as ammonium heptamolybdate, chemical formula: $(NH_4)_6Mo_7O_{24}$) has chemical properties like white crystalline powder; solubility in water; insolubility in alcohol; nonflammability. It is made by dissolving molybdenum trioxide in a large volume of aqueous ammonia and then evaporating the solution at room temperature. It is used as an analytic reagent for determining the content of phosphates, silicates, arsenates, and lead; for the production of molybdenum metal and ceramics; for the production of dehydrogenation and desulphurization catalysts; for the fixing of metals; for electroplating; as a

crop fertilizer supplement; as a negative stain in biological electron microscopy; and as an analgesic in medicine [79].

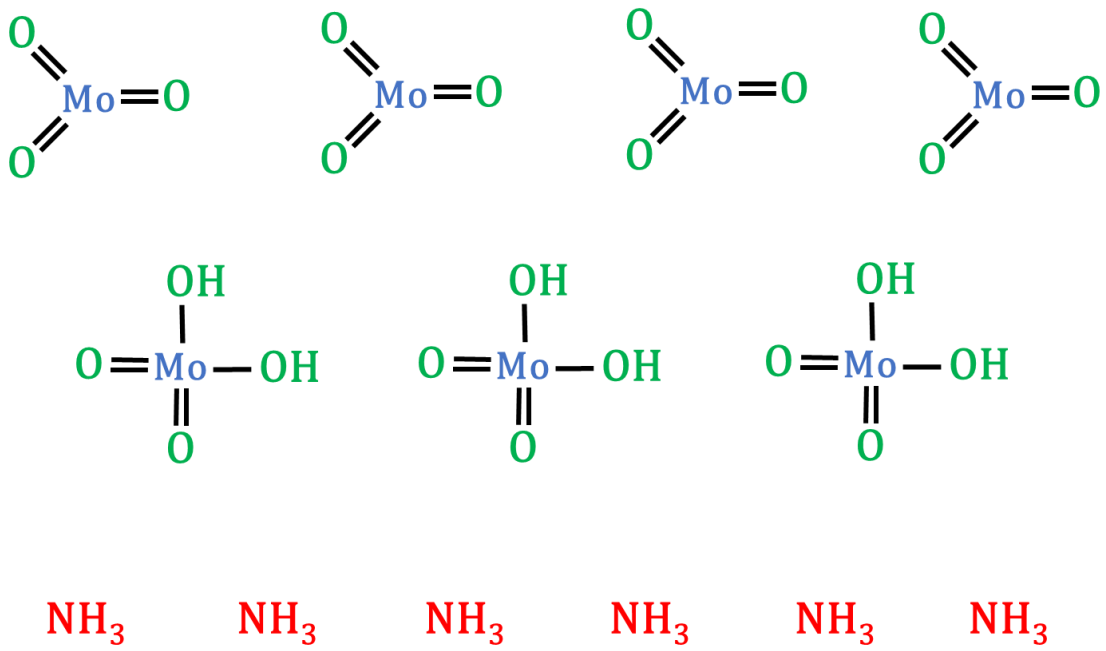

Figure 5: Atomic structure of Ammonium Molybdate {$(NH_4)_6Mo_7O_{24}$}

Chapter 3: Sensor Fabrication and Morphological Studies

3.1 Composition of Phosphate Solutions

All the chemical solutions were bought from EMD Millipore like- Potassium phosphate monobasic (ACS reagent, ≥99.0%), Potassium phosphate dibasic (ACS reagent, ≥98%), Sodium phosphate monobasic (BioXtra, ≥99.0%), Sodium phosphate dibasic (BioXtra, ≥99.0%). Using the deionized water produced in our Biosensor and BioMEMS Lab, UWM, all the salts were converted into different concentrated solutions. With molecular weights for KH_2PO_4 (136.09 g/mol), K_2HPO_4 (174.18 g/mol), NaH_2PO_4 (119.98 g/mol) and Na_2HPO_4 (141.96 g/mol), different amount of DI water was taken into mass cylinder according to the concentration range from 10^{-11} to 10^{-2} (mol/L) and Analytical Balance (120 g x 0.1 mg).

3.2 Synthesis of Pyrrole and Ammonium Molybdate Nanocomposite

Both Pyrrole (reagent grade, 98%) and Ammonium molybdate (99.98% trace metals basis) were purchased from the EMD Millipore. With having molecular weights of 67.09 g/mol (for Pyrrole) and 196.01 g/mol (for Ammonium molybdate), the solutions were made using the deionized water. An analogous mixture of 0.2 M Py (Pyrrole) and $2x10^{-3}$ M AM (Ammonium molybdate) were made as drop casting solutions.

3.3 Pretreatment of Sensor Electrodes

Before the surface modification of the working electrode, all of the new bare SPE sensors were cleaned. By cyclic voltammetry (0.0 to 1.4 V, 15 cycles, scan rate 50 mV/s), the new SPE was cleaned with 0.1 M H2SO4 solution, followed by soaking (just the electrode section) in 0.1 M NaCl solution and then acetone for 1 minute each to remove any physically adsorbed

contaminants on the electrode surface. Using a squeeze wash bottle, the SPE was cleansed in fresh DI water between each cleaning procedure. All of the sensors were cleaned and dried at room temperature for 8 hours before being treated.

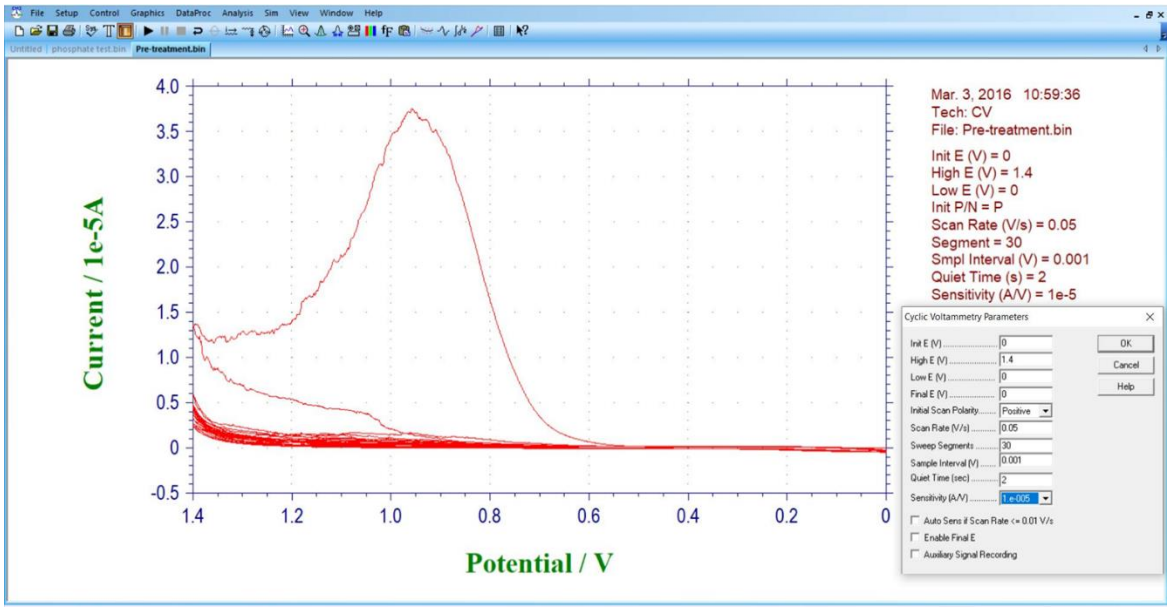

Figure 6: Cyclic voltammetry (CV) technique used for pretreatment using the electrochemical station

3.4 Modification of Working Electrode Surface

The working electrode of the SPE sensor was modified with a homogeneous mixture of 0.2 M Py (pyrrole) and $2x10^{-3}$ M AM (ammonium molybdate). Experimentally, the optimal concentrations of these elements were calculated. To modify the surface of the working electrode, 8 µL of the mixture were drop casted on it and dried at room temperature for 24 hours. Before testing with the analytical solution, all of the fabricated sensors were washed with DI water (dip method) to eliminate any physically adsorbed nanocomposite film or loose particle.

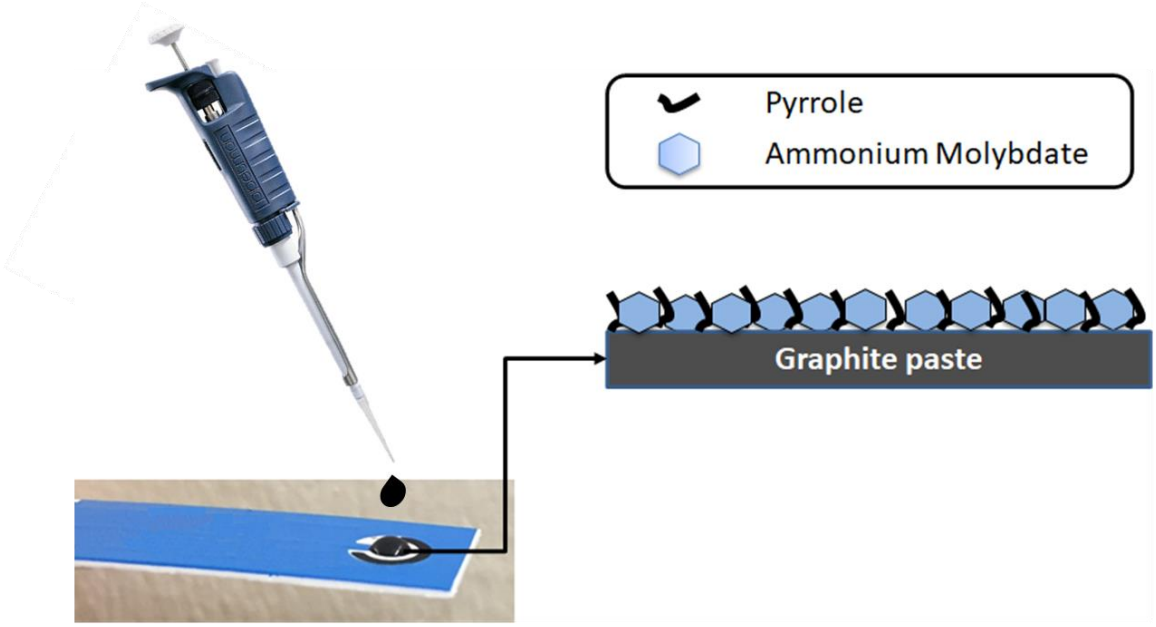

Figure 7: Synthesis of Py-AM nanocomposite

3.4 Phosphate Detection Analysis

The content of phosphate in the sample solution was determined using open circuit voltammetry. The potential response from the SPE phosphate sensor was recorded using the three-electrode system at room temperature utilizing the CHI-6012E electrochemical analyzer. The potential is measured in open circuit voltammetry when there is no external current flowing in the system. After encountering phosphate solution, the creation of phosphate complexes on the SPE sensor causes a potential change. Figure 8 depicts a schematic of the developed phosphate sensor's measurement technique.

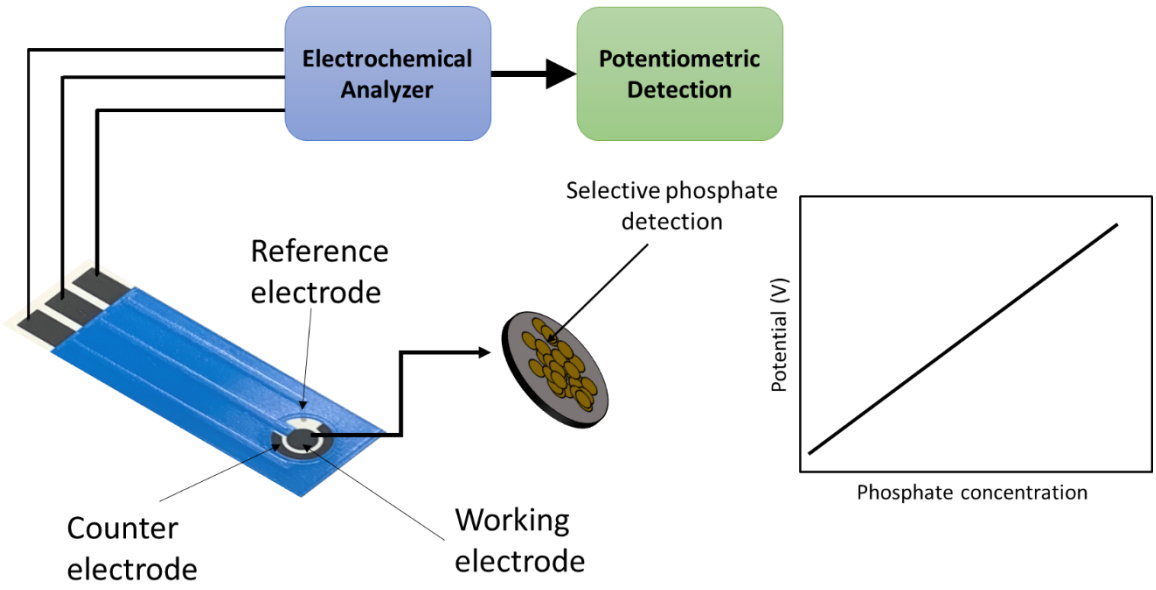

Figure 8: Schematic of phosphate sensing using electrochemical method

Various concentrations of phosphate were tested with the built SPE sensor for electrochemical detection of phosphate anions. The designed phosphate sensor was tested using the dipping method. For the open circuit time potential research, the sensor was immersed in the sample solution. At room temperature, the testing lasted 400 seconds and data was recorded every 0.1 second. For a consistent phosphate concentration in the sample vial, a magnetic stirrer was utilized at 750 rpm. Averaging the measured values from 180s to 300s yielded the concentration.

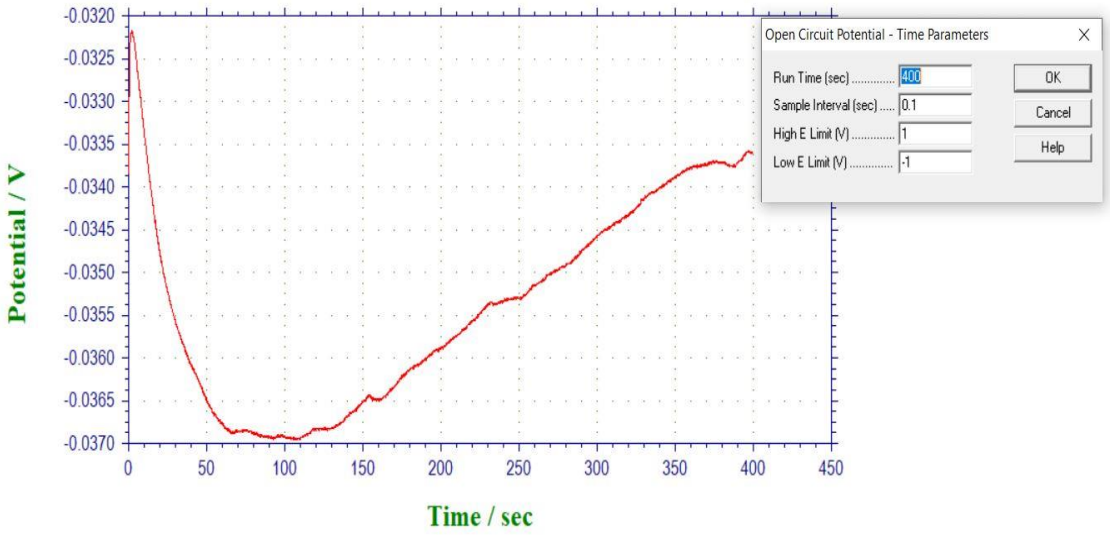

Figure 9: OCPT reading of a single measurement with a phosphate sensor

3.4 Surface Morphology Study for Nanocomposite Film

The surface morphology of the bare SPE's working electrode, Py-AM modified working electrode (before use), Py-AM modified working electrode (after use), were characterized by scanning electron microscopy (SEM) image.

3.4.1 SEM image for uncoated or Bare Sensor (no extra nanomaterials)

Figure 9 shows a SEM image of the SPE's uncoated (no extra nanomaterials) working electrode. The working electrode is made of graphite powder, as indicated in material and instruments section.

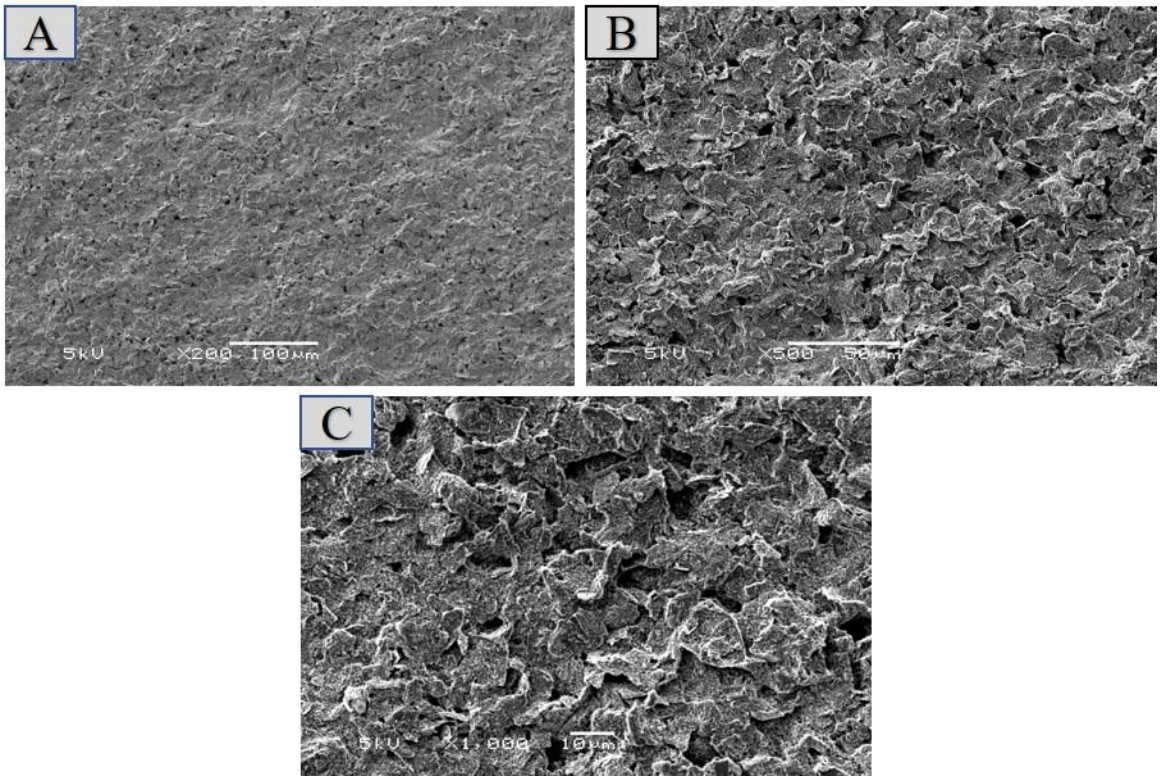

Figure 10: Scanning electron microscopy (SEM) images of bare SPE (A) x200 magnification (left)(B) x500 magnification (C) x1000 magnification

The bare sensor showed the porous layered structure of carbon. The surface is not smooth and there are plenty of holes in the surface of the working electrode.

3.4.2 SEM image for PY-AM nanocomposite modified sensor

Figure 11 illustrates the SEM images when the working electrode is fabricated with the proposed drop casting material. So, after adding the nanocomposite materials (Py and AM), the working surface is analyzed using the SEM images.

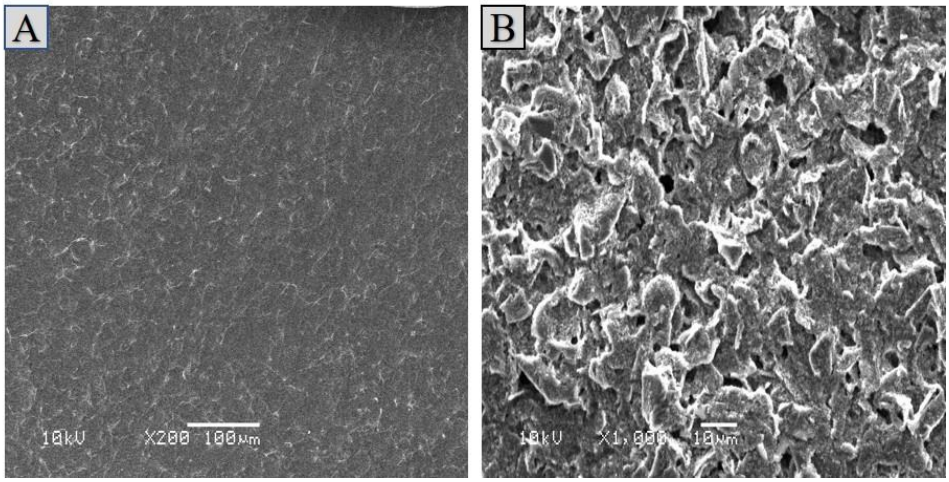

Figure 11: Scanning electron microscopy (SEM) images of AM-PY modified SPE (A) before experiment x200 magnification (B) before experiment x1000 magnification

The crumpled layers of the AM-pyrrole nanocomposite have enhanced the surface area of the carbon electrode as compared to the bare electrode, as illustrated in Fig. 10. Without precipitation, the colorless AM blended effectively with the pyrrole solution. On the SPE's carbon working electrode, the stable structure created a light grey coating. The layer of the AM and pyrrole combination does not display any cracks, as seen in Figs. 11A and 11B, indicating a solid bond with the carbon electrode.

3.4.3 SEM image for modified sensor after using in Sodium Phosphate Solutions

Figure 11 discusses the after effect of the surface of the working electrode. Both NaH_2PO_4 and Na_2HPO_4 solution has been used to see the surface status of the electrode when the electrochemical analysis is done.

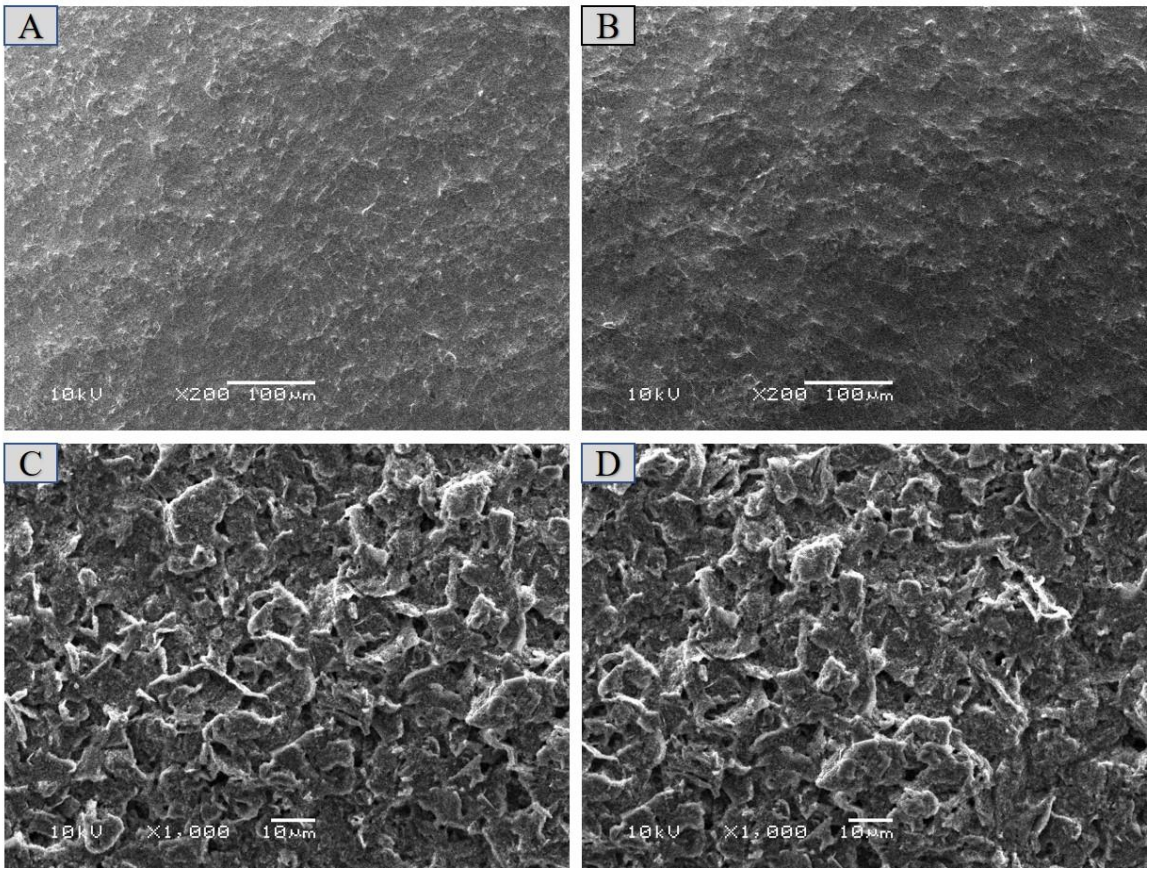

Figure 12: Scanning electron microscopy (SEM) images (A) after experiment x200 magnification in NaH_2PO_4 (B) after experiment x200 magnification in Na_2HPO_4 (C)after experiment x1000 magnification in NaH_2PO_4 (D) after experiment x1000 magnification in Na_2HPO_4

Even after utilizing the sensor to detect varying concentrations of phosphate in water, there is no obvious degradation or physical change to the AM-pyrrole structure (Fig. 12A, B, C, D). The color has lightened due to the removal of molybdate components from the carbon substrate.

3.4.4 SEM image for modified sensor after using in Potassium Phosphate Solutions

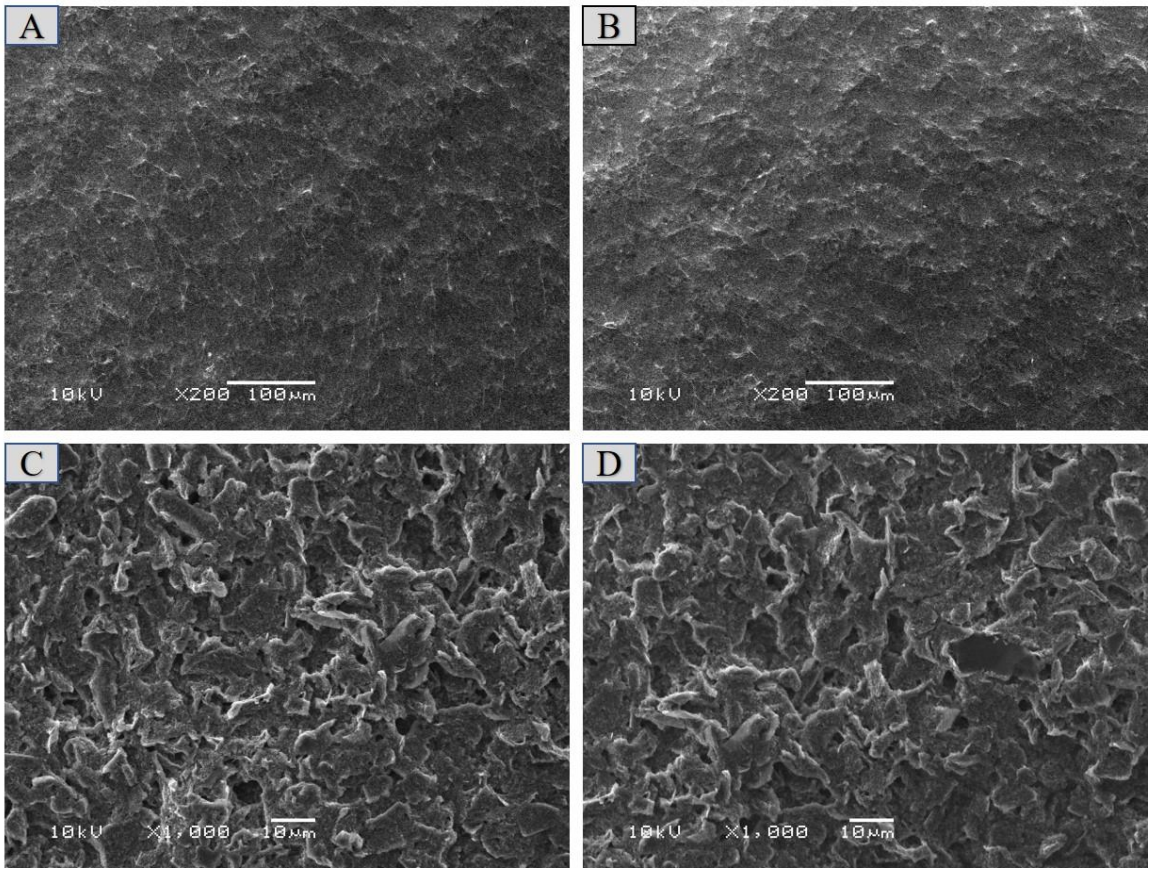

Figure 13: Scanning electron microscopy (SEM) images (A) after experiment x200 magnification in KH_2PO_4 (B) after experiment x200 magnification in K_2HPO_4 (C)after experiment x1000 magnification in KH_2PO_4 (D) after experiment x1000 magnification in K_2HPO_4

For the surface study, both KH_2PO_4 and K_2HPO_4 solution have been utilized similar to the previous one to determine the surface status of the electrode. No significant crack or rupture has been observed from the morphological analysis on Figure 13.

Chapter 4: Result & Performance Analysis

4.1 Measurement of Phosphate ion

Phosphate ($H_2PO_4^-$ & HPO_4^-) solutions with concentrations ranging from 10^{-11} to 10^{-2} (mol/L) were utilized to determine the sensitivity and lower detection limit of the proposed sensor. The content of phosphate was measured using the electrical potential established by open circuit voltammetry. Both the monobasic and dibasic solutions of phosphate were used to determine the phosphate level in the aqueous solution. The potential response from the SPE phosphate sensor was recorded using the three-electrode system at room temperature utilizing the CHI-6012E electrochemical analyzer. The potential is measured in open circuit voltammetry when there is no external current flowing in the system. After encountering phosphate solutions, the creation of phosphate complexes on the SPE sensor causes a potential change.

4.2 Open circuit voltammetry analysis with Sodium Phosphate solutions

Both NaH_2PO_4 (Monosodium phosphate, also known as monobasic sodium phosphate and sodium dihydrogen phosphate) and Na_2HPO_4 (Disodium phosphate, or sodium hydrogen phosphate, or sodium phosphate dibasic) solutions were used for the determination of phosphate ions. Potential Vs. Time (V-t) response were taken and analyzed later for different concentration and also with different conditions.

4.2.1 V-t response for NaH_2PO_4 Standard Solution

As discussed before, different concentration with a range from 10^{-11} to 10^{-2} (mol/L) were made using NaH_2PO_4 Standard Solution and the sensors were tested maintaining different criteria. The range from 10^{-11} to 10^{-2} (mol/L) was divided into half. The first half (ranging from 10^{-11} to 10^{-}

^{7} (mol/L)) was tested with a single sensor. The other half of the concentration was tested with the same sensor. Both the raw data and statistical data were analyzed using CHI-6012E electrochemical analyzer's inbuilt graph software, Microsoft excel and Origin software.

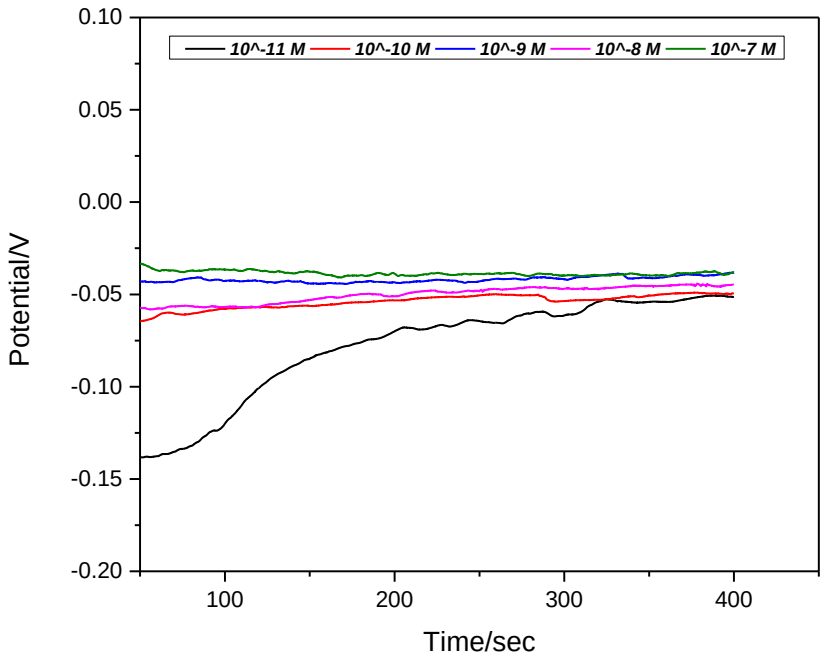

Figure 14: Raw Data Analysis of phosphate detection using NaH_2PO4 Standard Solution (with a range from 10^{-11} to 10^{-7} (mol/L))

Figure 14 depicts graph of a single calculation of a Py-AM modified screen-printed electrode. The sensor was washed with deionized water before dipping in the phosphate solutions. The first concentration of the NaH_2PO_4 Standard Solution was 10^{-11} (mol/L). It is the lowest detection limit that the sensor can detect phosphate properly. From the start of the voltammetry process until 200 second, a fluctuation is seen from the graph. It is because the sensor takes some time at beginning to get stabilized with the solution environment and after that it shows linear progress until the last second of the experiment. Gradually the concentration where increased 10 times from the previous

one and the sensor was tested with each of them. In between each of the test, the sensor was washed carefully with the deionized water to remove any solution left from the previous detection. From the Figure 14, it can be clearly stated that, the sensor has shown linear potential response from low to high concentration of phosphate solutions. It shows that the sensor has reusability factor and using different concentration with the same sensor do not affect the working performance which the potential response of detecting phosphate in aqueous solutions.

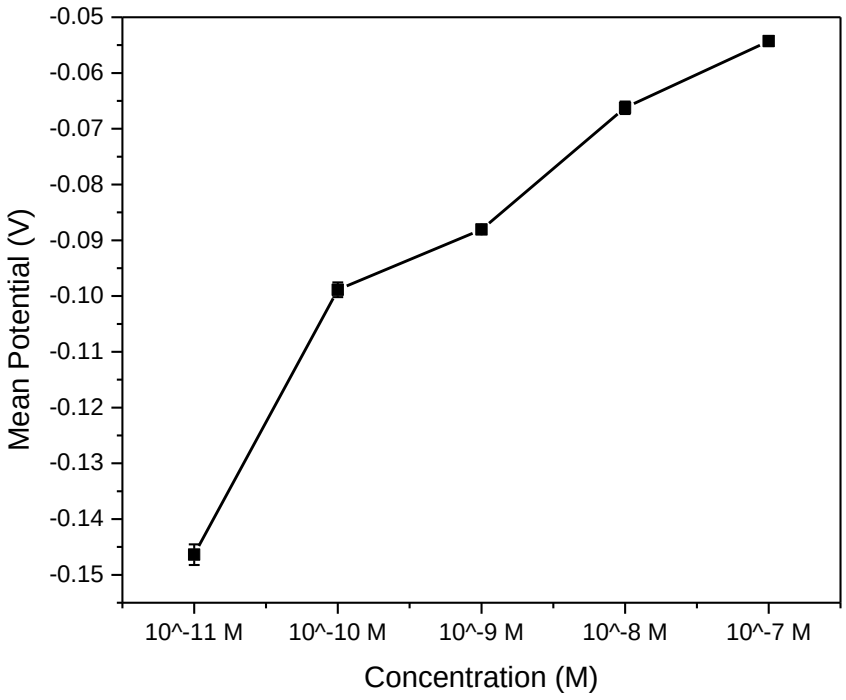

Figure 15: Statistical Analysis of phosphate detection using NaH_2PO4 Standard Solution (with a range from 10^{-11} to 10^{-7} (mol/L))

Statistical data including mean value and standard deviation was analyzed for each of the concentration using the Origin software. As discussed before, it takes some seconds for the senor to get stand with the solution environment. After stabilization, the electrical potential of each phosphate concentration was calculated by averaging measured values from 180 to 300 seconds.

Stabilization takes about 1 minute on average. The first concentration (10^{-11} (mol/L)), the standard deviation value was ±0.00186. It is greater than the other concentration's standard deviation values because the sensor takes some time to show linear response with respect to the conditions. The fluctuation occurs due to the unstable condition during the first couple of seconds. As a result, the potential response for the first concentration deviates a little more than the remaining concentrations that are tested with the same sensor. From Figure 15, it can be easily summarized that, the potential response increment was in proportion as the phosphate concentration was increased.

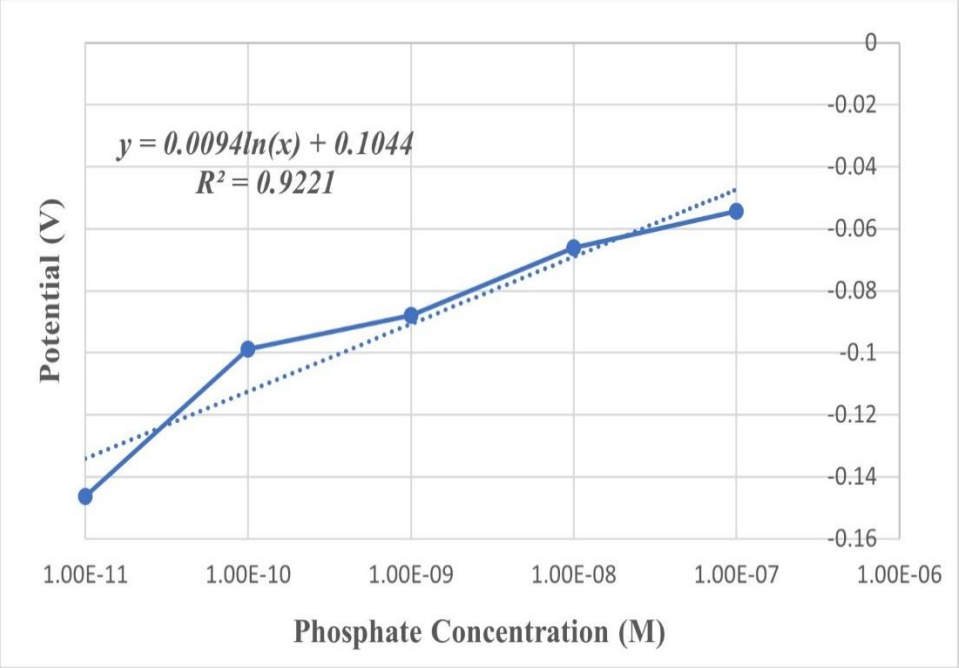

Figure 16: Linear Regression of phosphate detection using NaH_2PO4 Standard Solution (with a range from 10^{-11} to 10^{-7} (mol/L))

The OCPT response for the lower range of phosphate concentration has shown improved calibration curve (logarithmic fit). From Figure 16, the linear regression for the range 10^{-11} to 10^{-}

^{7} (mol/L)) has been plotted. With a R^2 value of 0.9221, it can be easily outlined that the proposed sensor has great capability of detecting phosphate.

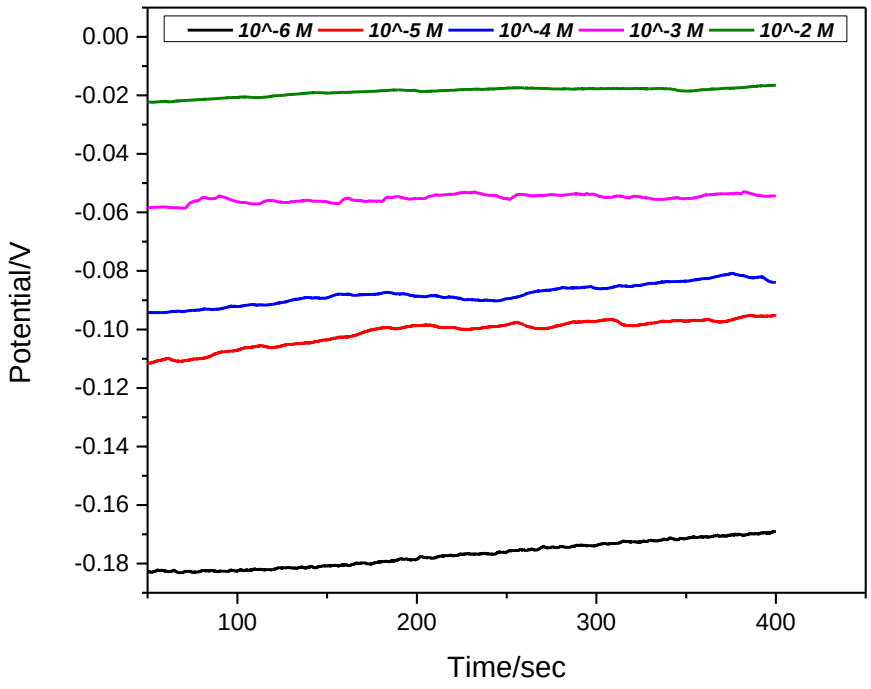

Figure 17: Raw Data Analysis of phosphate detection using NaH_2PO4 Standard Solution (with a range from 10^{-6} to 10^{-2} (mol/L))

As discussed before, the last half of the concentration range from 10^{-6} to 10^{-2} (mol/L) were tested with the same sensor that was used previously. Figure 17 depicts graph of a single calculation of a Py-AM modified screen-printed electrode. The first concentration of the NaH_2PO_4 Standard Solution was 10^{-6} (mol/L). The concentration was then gradually increased 10 times up to 10^{-2} (mol/L). It showed good linearity until the highest concentration that our sensor can detect and none of the curve overlapped with each other. So, the potential response for all of the concentration throughout the 400 seconds did not intersect with each other.

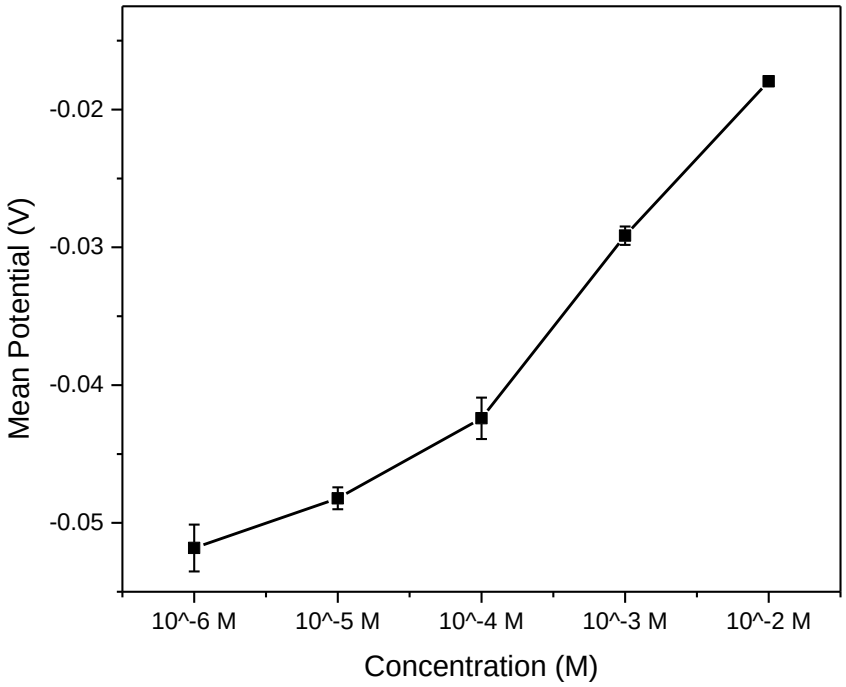

Figure 18: Statistical Analysis of phosphate detection using NaH_2PO_4 Standard Solution (with a range from 10^{-6} to 10^{-2} (mol/L))

Statistical data including mean value and standard deviation was analyzed for each of the concentration ranging from 10^{-6} to 10^{-2} (mol/L). For the first concentration (10^{-6} (mol/L)), the standard deviation value was ± 0.0017 and it is the highest variance among other deviations of the concentration. Taking the average data for 180-300 seconds, from Figure 18, it can be easily indicated that like the lower concentration set, the higher concentrations also showed good linear potential response in respect to the rise of concentration limit.

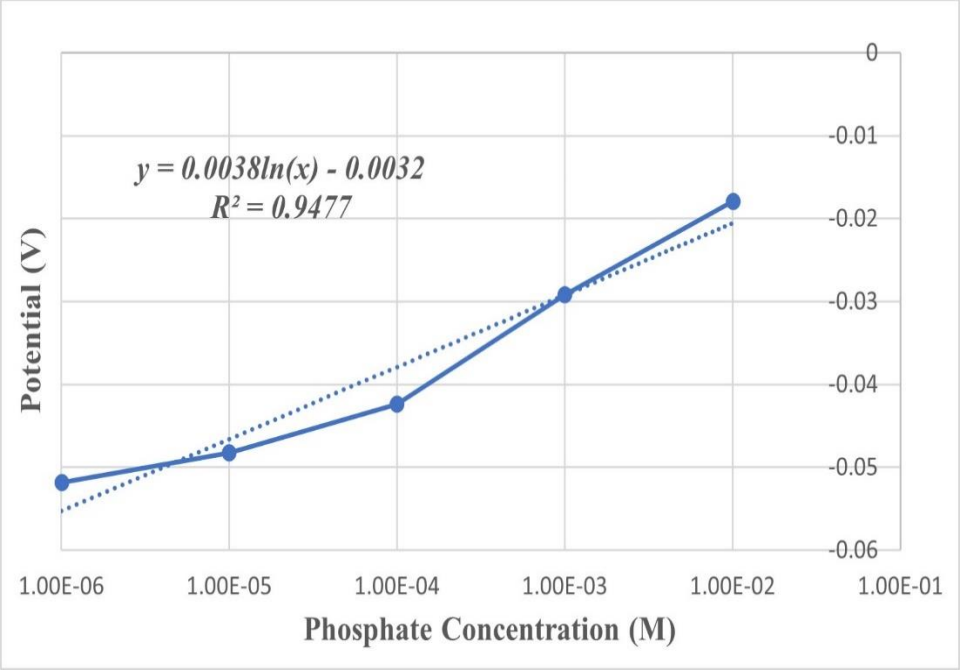

Figure 19: Linear Regression of phosphate detection using NaH_2PO_4 Standard Solution (with a range from 10^{-6} to 10^{-2} (mol/L))

Figure 19 displays the OCPT response for the higher range of phosphate concentration. With a R^2 value of 0.9477 and improved calibration curve (logarithmic fit), the detection capability of phosphate in higher range of concentration can be proved.

4.2.2 V-t response for Na_2HPO4 Standard Solution

Same as before, different concentration with a range from 10^{-11} to 10^{-2} (mol/L) were made using Na_2HPO_4 Standard Solution to test with the developed sensor. The first half (ranging from 10^{-11} to 10^{-7} (mol/L)) and the other half of the concentration was tested with same sensor. Both the raw data and statistical data were analyzed using CHI-6012E electrochemical analyzer's inbuilt graph software and Origin software. Microsoft Excel was used for plotting linear regression curve.

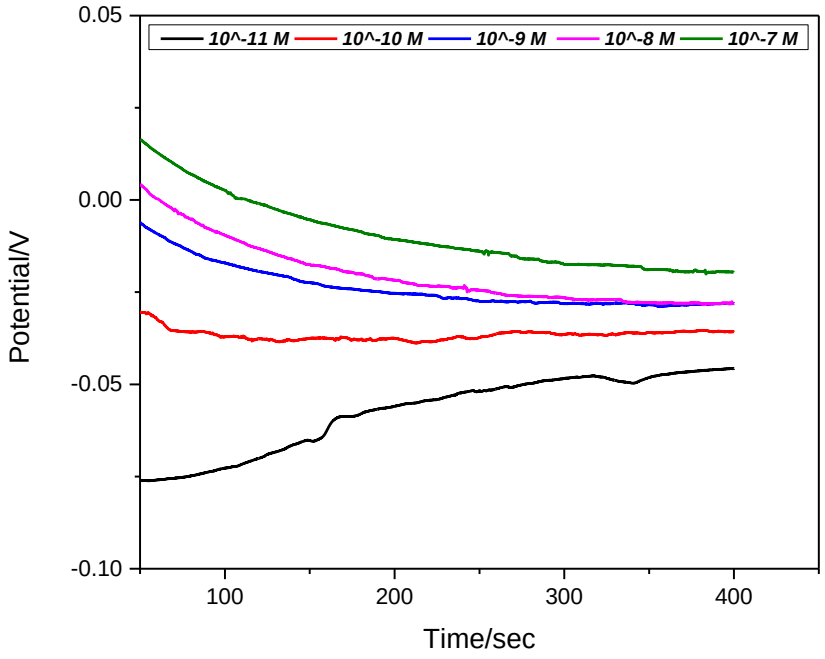

Figure 20: Raw Data Analysis of phosphate detection using Na_2HPO_4 Standard Solution (with a range from 10^{-11} to 10^{-7} (mol/L))

The above is a raw data an individual sensor modified with of a Py-AM based nanocomposite. The sensor was washed with deionized water before dipping in the phosphate solutions. The first concentration of the Na_2HPO_4 Standard Solution was 10^{-11} (mol/L) which is the lowest concentration that our sensor can detect properly. Same as sodium monobasic concentrated solutions, the first curve has a little bit of seesawing at the beginning. But the fluctuation got stable after a certain time, and it remained stabilize until the end. Concentrations were gradually increased 10 times for each measurement and the sensor displayed better feedback until last concentration.

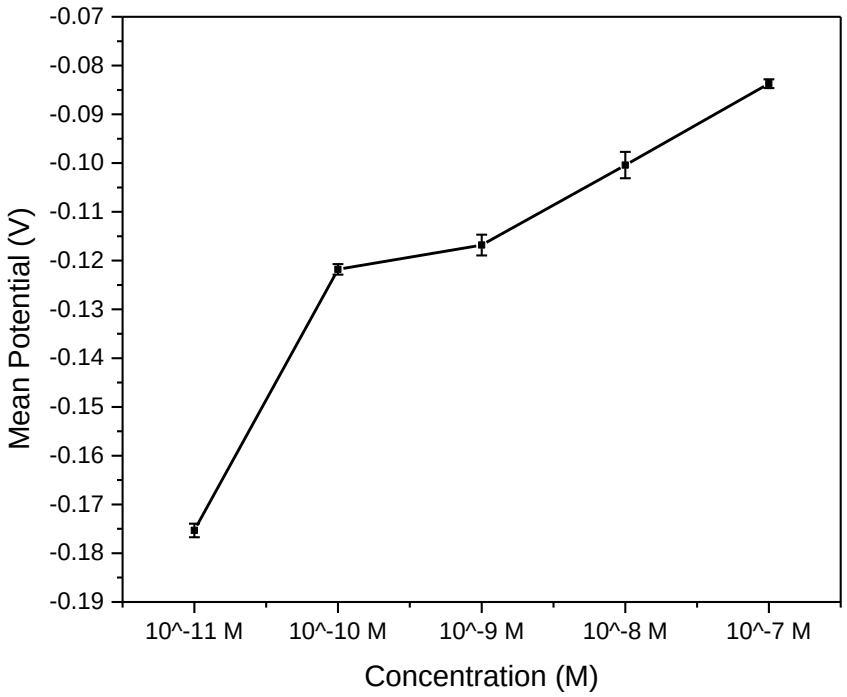

Figure 21: Statistical Analysis of phosphate detection using Na_2HPO_4 Standard Solution (with a range from 10^{-11} to 10^{-7} (mol/L))

Using the Origin software, the average data taking from 180 second to 300 second was analyzed. Both the mean value with standard deviation was plotted on the above Figure 21. With the highest deviation value of ±0.00273 for the concentration 10^{-11} (mol/L), it can be stated that the sensor takes some time for stabilization at the beginning. With the lower error or deviation values for the later concentrations, it can be specified that the sensor shows appropriate linear response once it gets equilibrated.

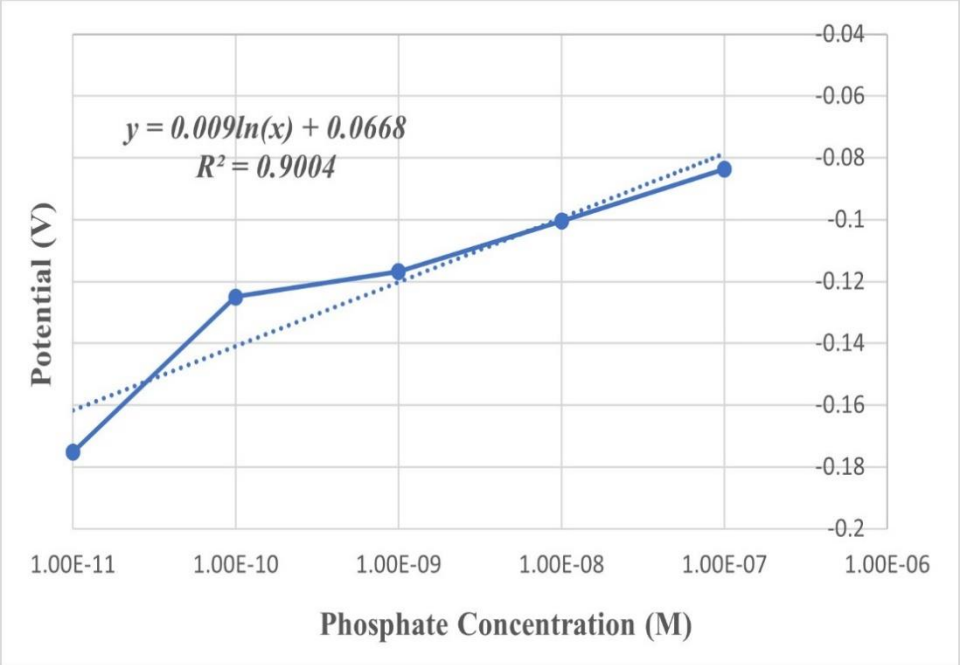

Figure 22: Linear Regression of phosphate detection using Na_2HPO_4 Standard Solution (with a range from 10^{-11} to 10^{-7}(mol/L))

Figure 22 displays the OCPT response for the range 10^{-11} *to* 10^{-7}*(mol/L)* of phosphate concentration. With a R^2 value of 0.9004 and improved calibration curve (logarithmic fit), the sensor has shown great character in terms of phosphate identification.

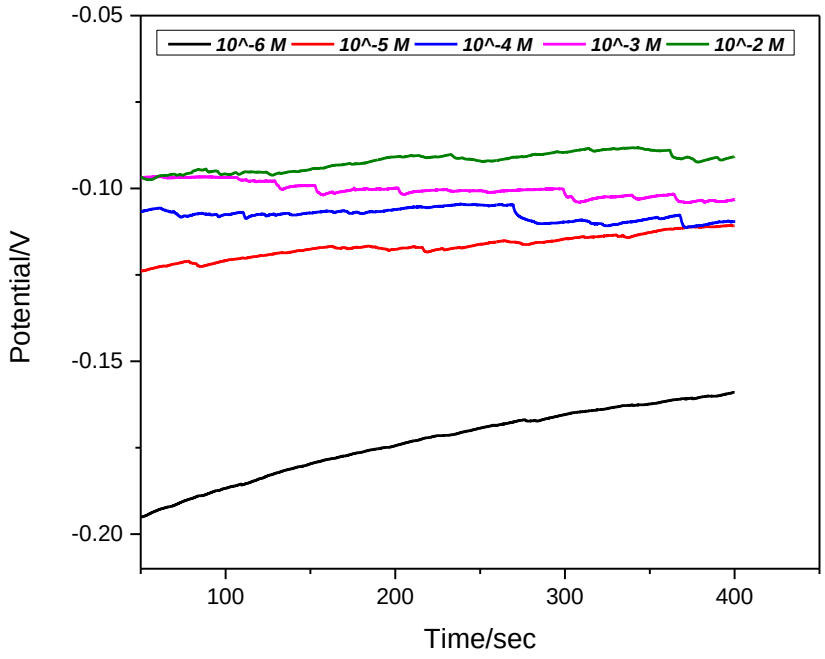

Figure 23: Raw Data Analysis of phosphate detection using Na_2HPO_4 Standard Solution (with a range from 10^{-6} to 10^{-2} (mol/L))

The detection test was started with 10^{-6} (mol/L) of Na_2HPO_4 Standard Solution which is the lower limit of the for this test. The potential response is quite a bit low in respect to the other higher concentration. Once the fluctuation period was over, increasing the concentration tenfold, did not affect the potential response of the sensor. Alike the sodium dibasic lower concentration range limit, the higher set of concentrations also indicated linear kind of potential response. It can be concluded that both for monobasic and dibasic solutions of sodium, our sensor has great prospects of sensing phosphate. Ranging the concentration in two different sets from high to low, the sensor has great characteristics in terms of potential feedback.

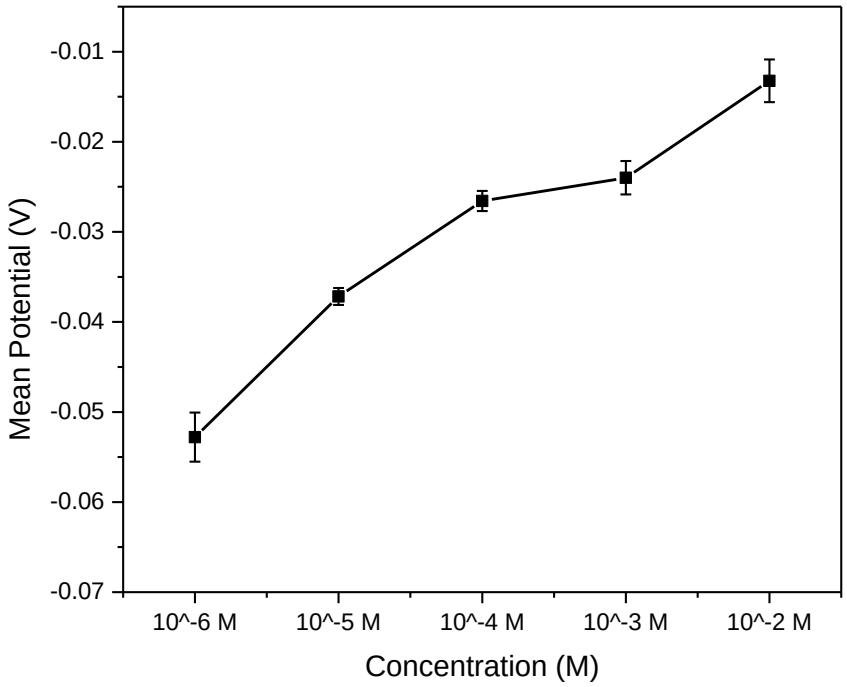

Figure 24: Statistical Analysis of phosphate detection using Na_2HPO_4 Standard Solution (with a range from 10^{-6} to 10^{-2} (mol/L))

The highest deviation was recorded for 10^{-6} (mol/L) and 10^{-2} (mol/L) respectively 0.0271 and 0.0212. Though inflated deviation was acquired in the middle stage concentrations instead of the initial stage of test, the potential response was still linear regarding the increment of concentration.

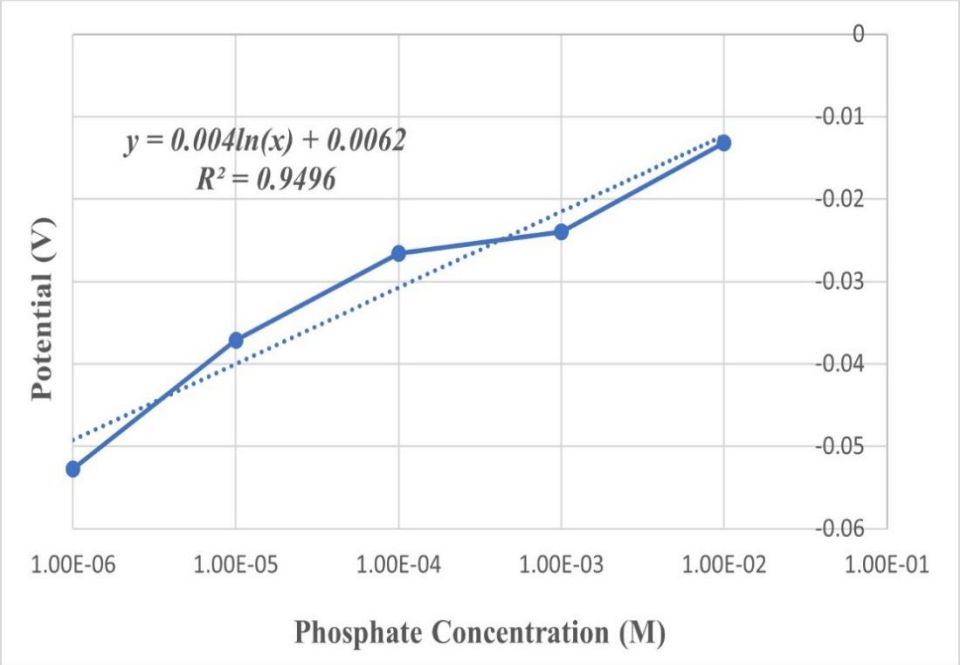

Figure 25: Linear Regression of phosphate detection using Na_2HPO_4 Standard Solution (with a range from 10^{-6} to 10^{-2}(mol/L))

Figure 25 displays the OCPT response for the range 10^{-6} to 10^{-2}(mol/L) of phosphate concentration. With a R^2 value of 0.9496, the logarithmic fit indicated remark of good calibration result. From the above results, it can be concluded that for a vast range from 10^{-11} to 10^{-2} (mol/L), Na_2HPO_4 has shown enhanced performance in terms of phosphate detection.

4.3 Open circuit voltammetry analysis with Potassium Phosphate solutions

Both KH_2PO_4 (Monopotassium phosphate, also known as monobasic potassium phosphate and potassium dihydrogen phosphate) and K_2HPO_4 (Dipotassium phosphate, or potassium hydrogen phosphate, or potassium phosphate dibasic) solutions were used for the determination of phosphate ions. Potential Vs. Time (V-t) response were taken and analyzed later for different concentration and also with different conditions.

4.2.1 V-t response for KH_2PO_4 Standard Solution

Various concentrations with a range from 10^{-11} to 10^{-2} (mol/L) were produced using KH_2PO_4 Standard Solution and the sensors were tested maintaining different criteria. The range from 10^{-11} to 10^{-2} (mol/L) was separated into two halves. Both the first half (ranging from 10^{-11} to 10^{-7} (mol/L)) and the other half (ranging from 10^{-6} to 10^{-2} (mol/L)) of the concentration were tested with the same sensor. CHI-6012E electrochemical analyzer's inbuilt graph software was used for raw data analysis, Microsoft excel, and Origin software were used for statistical plotting.

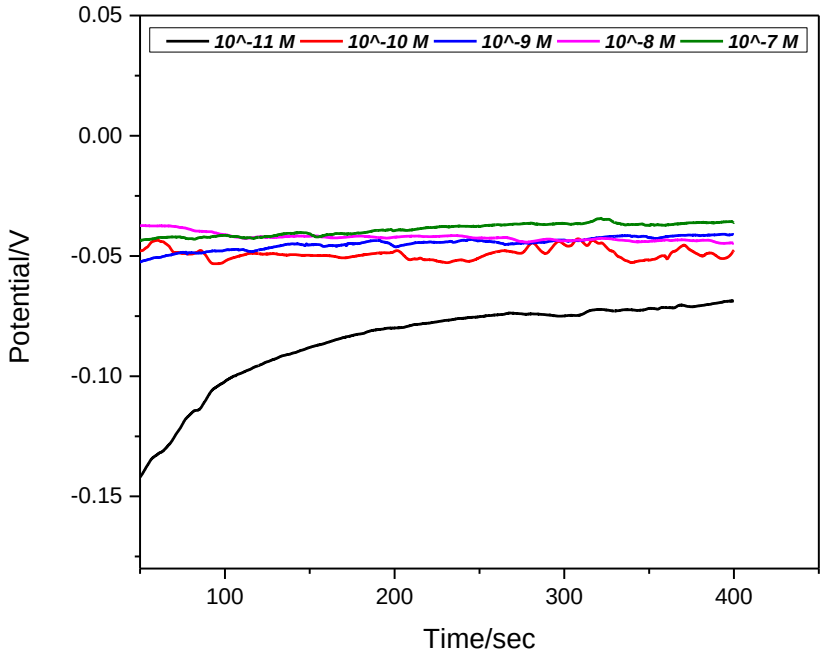

Figure 26: Raw Data Analysis of phosphate detection using KH_2PO_4 Standard Solution (with a range from 10^{-11} to 10^{-7} (mol/L))

Figure 26 depicts graph of a sole computation of a Py-AM modified screen-printed electrode. Using the deionized water, the sensor was washed properly at starting to avoid any unwanted particle on the drop-casting surface. The first concentration of the KH_2PO_4 standard solution was

10^{-11} (mol/L). As considered before, the first electrochemical analysis always experiences some fluctuation. The sensor needs some seconds to get adapted with the concentration effect. With a gradual increment of 10 times from the previous one and the sensor was tested with each of them. In between each of the test, the sensor was washed carefully with the deionized water to remove any solution or particle left from the previous detection. From the Figure 26, the potential response for 10^{-8} (mol/L) and 10^{-9} (mol/L) has overlapped with each other in some point but the voltage was higher for 10^{-8} (mol/L) at an average. The voltage response for 10^{-10} (mol/L) also has some seesaw effect but still got moderate response. Linear potential response can be proved for low to high concentration of potassium phosphate solutions.

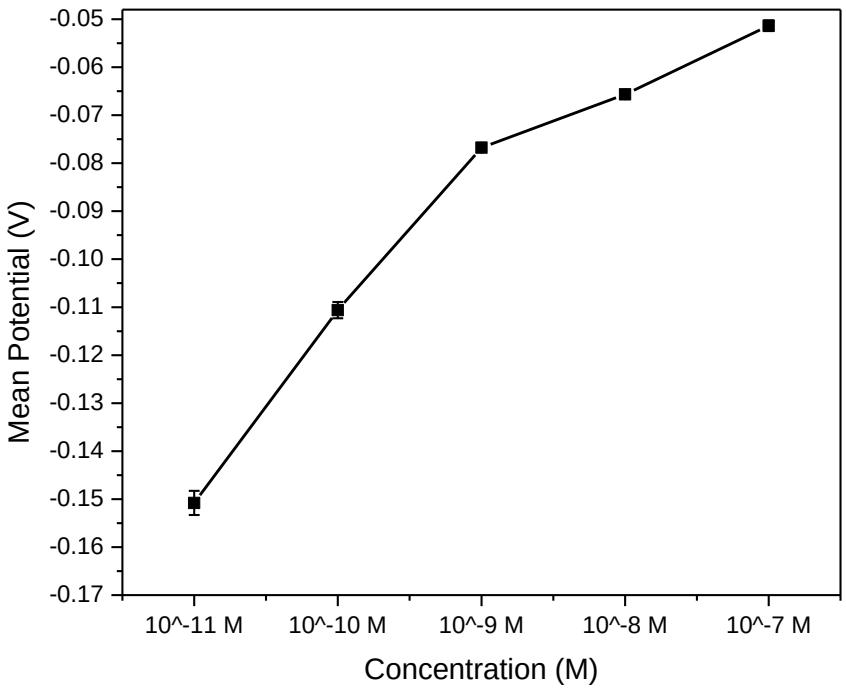

Figure 27: Statistical Analysis of phosphate detection using KH_2PO_4 Standard Solution (with a range from 10^{-11} to 10^{-7} (mol/L))

Using the Origin software, statistical data including mean value and standard deviation was analyzed for the potassium phosphate concentrations. From Figure 27, as there was fluctuation in the voltage response for the first concentration (10^{-11} (mol/L)), the standard deviation value was ±0.00252. It is higher than any other concentration's standard deviation values in the range. the same sensor. Same as the sodium phosphate solutions, the potassium phosphate solutions also had the potential response increment in proportion as the phosphate concentration was increased.

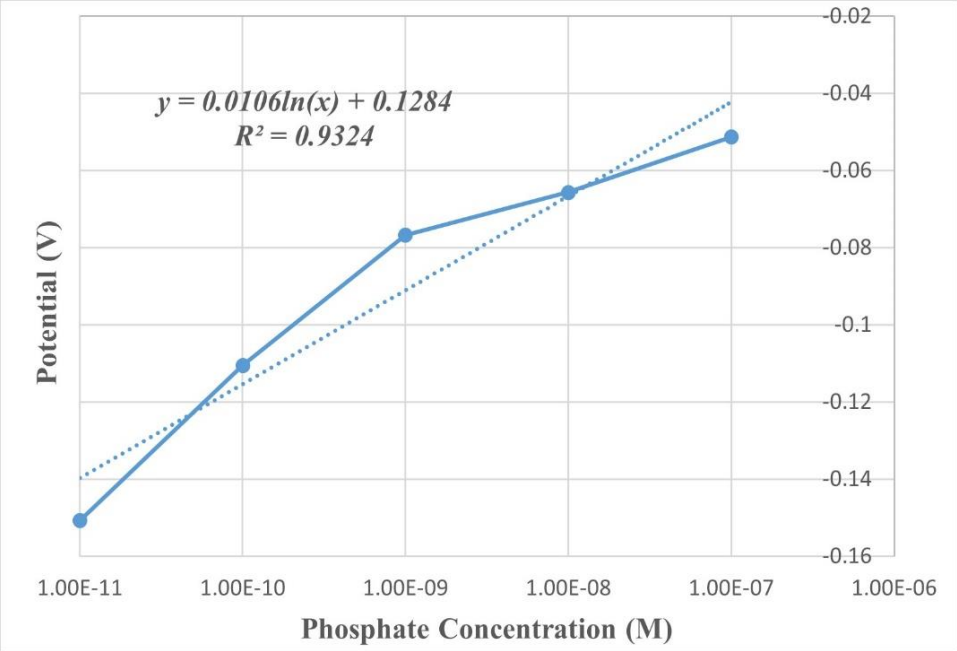

Figure 28: Linear Regression of phosphate detection using KH_2PO_4 Standard Solution (with a range from 10^{-11} to 10^{-7}(mol/L))

Figure 28 is the representation of the OCPT response for the range 10^{-11} to 10^{-7} (mol/L) of phosphate concentration. With a R^2 value of 0.9324, the logarithmic fit is a well portrayal of the calibration.

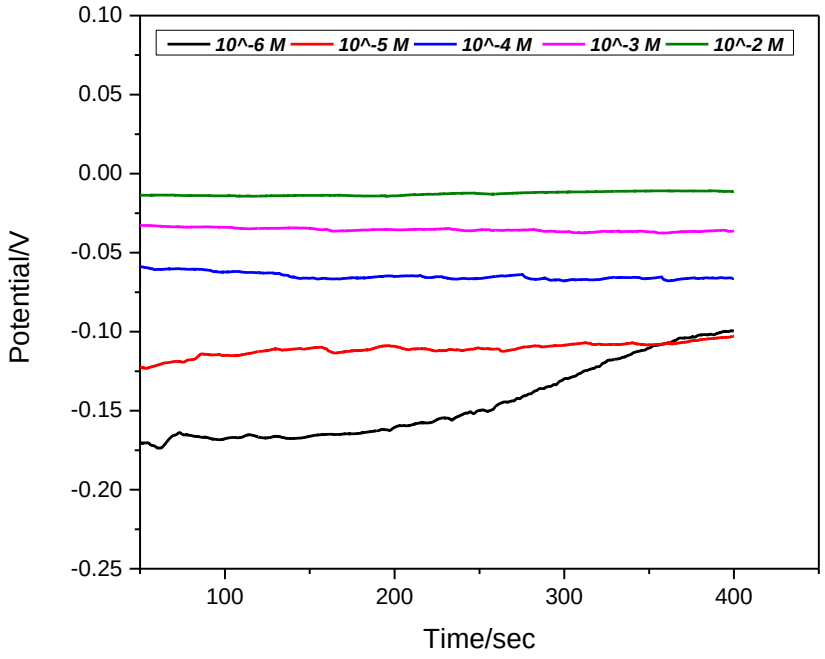

Figure 29: Raw Data Analysis of phosphate detection using KH_2PO_4 Standard Solution (with a range from 10^{-6} to 10^{-2} (mol/L))

The concentration ranges from 10^{-6} to 10^{-2} (mol/L) was tested with the previous Py-AM modified sensor. Figure 29 is the raw data for different concentrations of KH_2PO_4 standard solution. 10^{-2} (mol/L) is the highest limit for the detection. The lowest concentration which is 10^{-6} (mol/L) has overlapped with 10^{-5} (mol/L) concentration after 350 seconds until the end. On average, the potential value is still higher for 10^{-5} (mol/L) than the adjacent lower concentration.

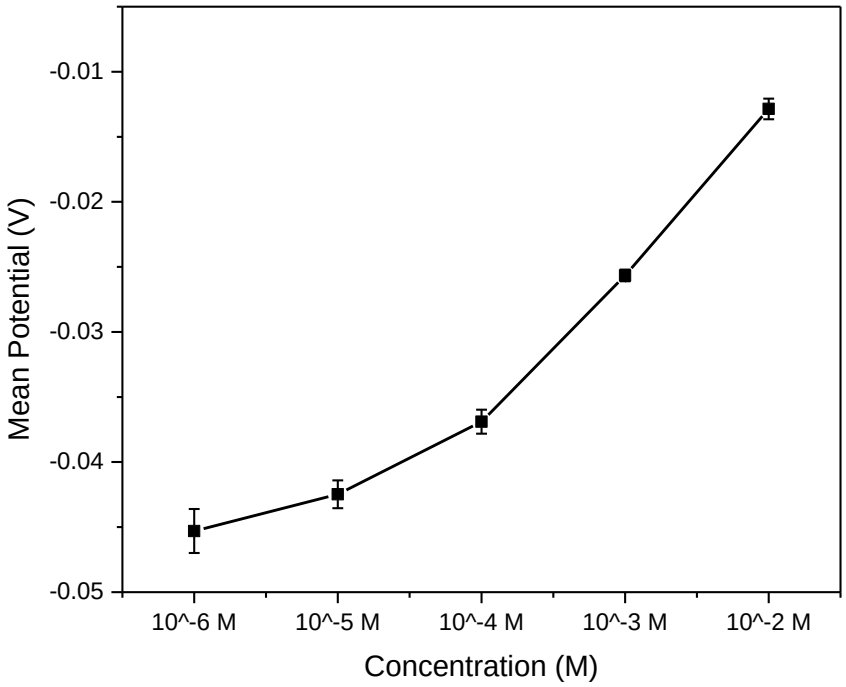

Figure 30: Statistical Analysis of phosphate detection using KH_2PO_4 Standard Solution (with a range from 10^{-6} to 10^{-2} (mol/L))

From Figure 30, the standard deviation value was ±0.00469 for the first concentration (10^{-6} (mol/L)). Though each of the concentration has got a little amount of deviation, the potential response was still proportional with the rise of phosphate concentrations.

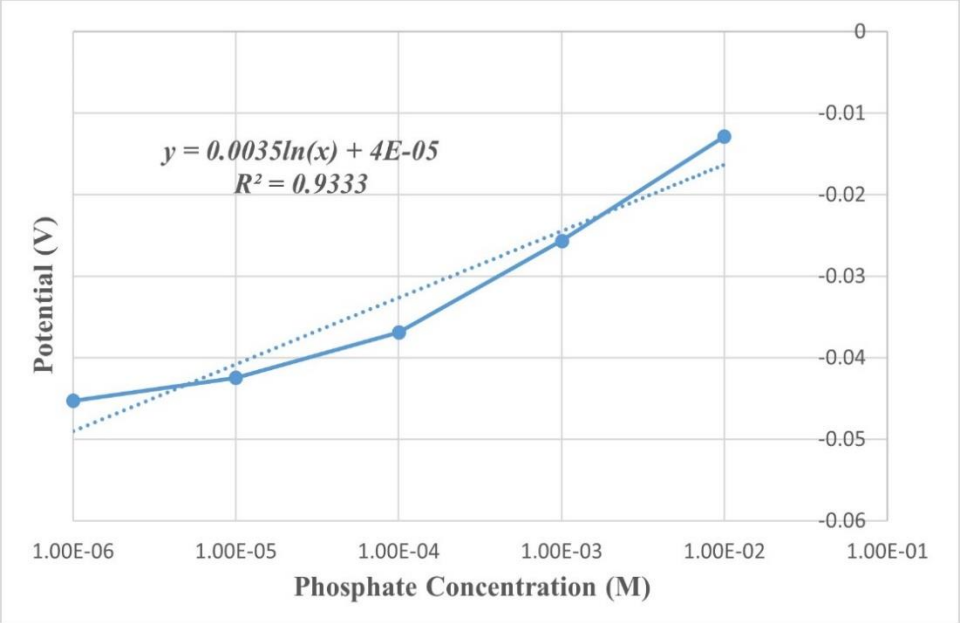

Figure 31: Linear Regression of phosphate detection using KH_2PO_4 Standard Solution (with a range from 10^{-6} to 10^{-2}(mol/L))

OCPT response for the range 10^{-6} to 10^{-2} (mol/L) of phosphate concentration has been shown in Figure 31. With a R^2 value of 0.9333, the logarithmic fit not only indicates excellent calibration but also high precision rate of phosphate detection. In finale, it can be validated that for an expansive range from 10^{-11} to 10^{-2} (mol/L), KH_2PO_4 has shown amplified performance in terms of phosphate detection.

4.2.2 V-t response for K_2HPO_4 Standard Solution

Like the previous experimentation, different concentration with a range from 10^{-11} to 10^{-2} (mol/L) were made using K_2HPO_4 standard solution to test with the proposed sensor. Two different sensors were used for 2 set of high and low range of the phosphate concentration. Later, the result was analyzed using different software.

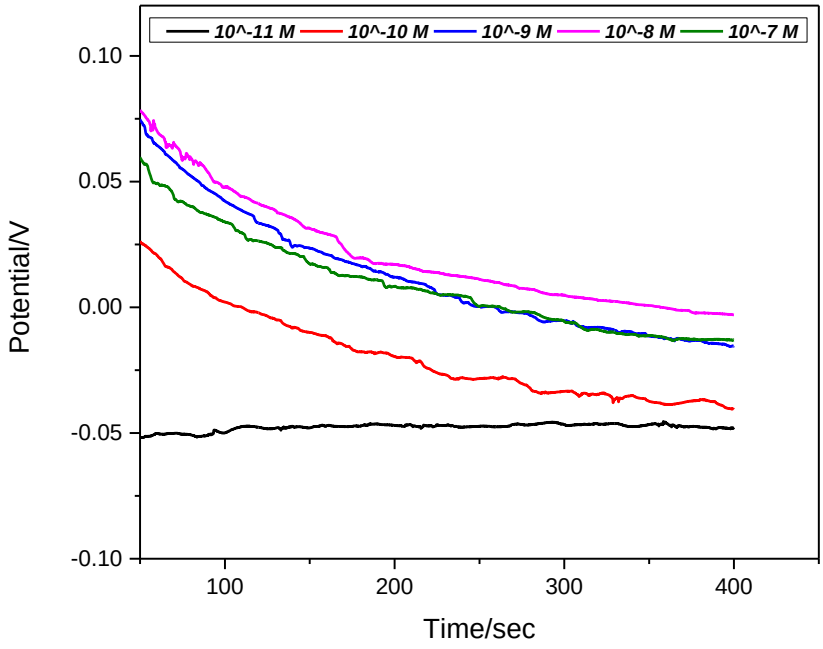

Figure 32: Raw Data Analysis of phosphate detection using K_2HPO_4 Standard Solution (with a range from 10^{-11} to 10^{-7} (mol/L))

Raw data an individual sensor fabricated with of a PY-AM based nanocomposite has been depicted in Figure 32. All the curves can be estimated in a way that at the beginning the sensor had unsaturated reading until 200 second. But the fluctuation got stable after that, and it remained stabilize until the end. Concentrations were gradually increased 10 times for each measurement and the sensor displayed finer feedback until last absorption.

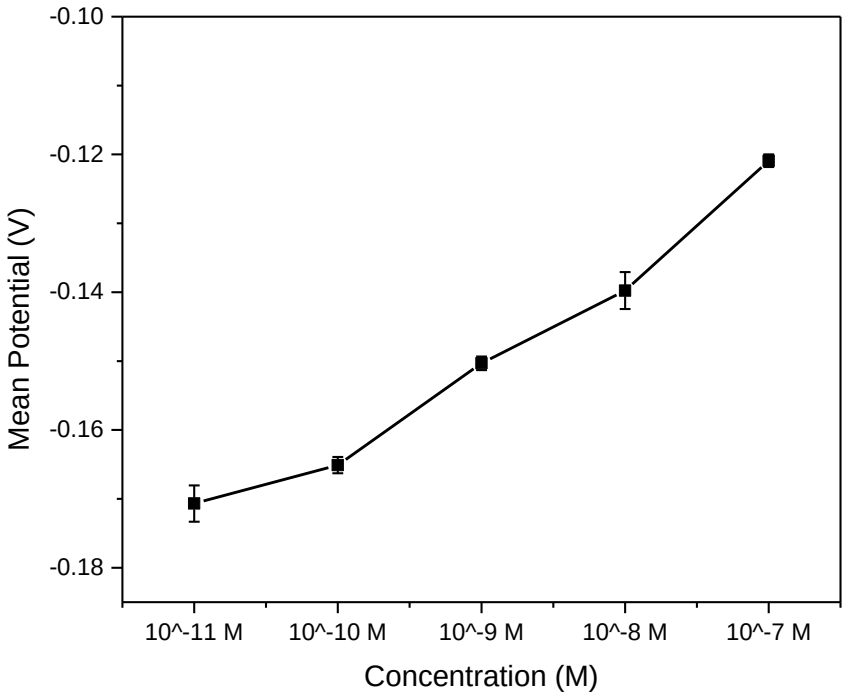

Figure 33: Statistical Analysis of phosphate detection using K_2HPO_4 Standard Solution (with a range from 10^{-11} to 10^{-7} (mol/L))

Keeping in mind the fluctuation, 180 second to 300 second was analyzed to get the average value for each of the concentration. The standard deviation range was within ±0.001 to ±0.002 for the last four concentrations. The first concentration 10^{-11} (mol/L) has very low deviation compared to the others. Still, the potential has risen with the enlargement of the phosphate concentrations.

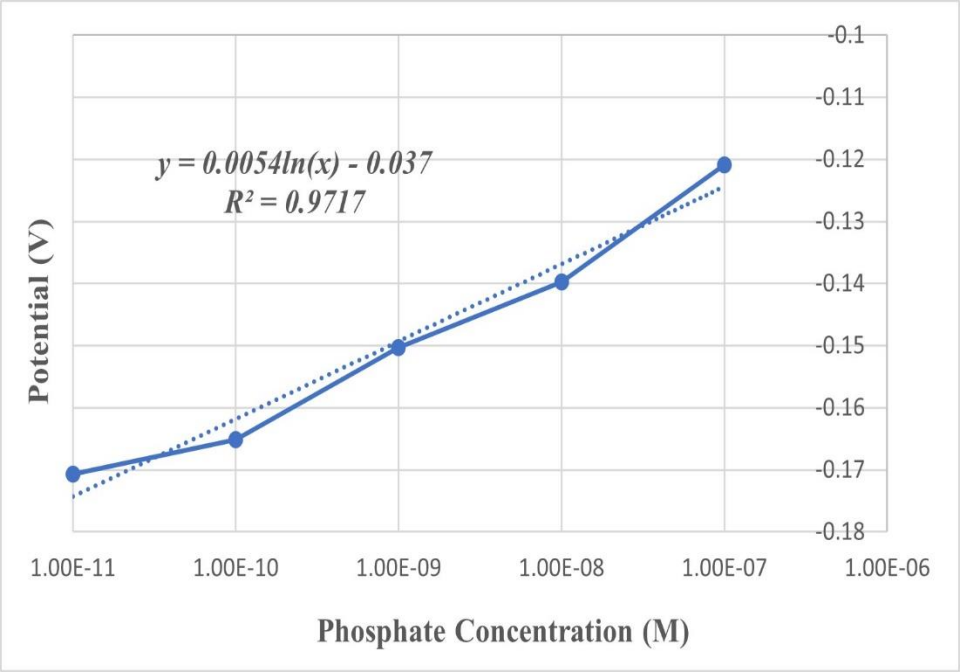

Figure 34: Linear Regression of phosphate detection using K_2HPO_4 Standard Solution (with a range from 10^{-11} to 10^{-7}(mol/L))

Figure 34 is the representation of linear regression plotting Potential (V) Vs. Phosphate Concentration (M) graph. With a $R^2 = 0.9717$, the logarithmic fit supports fully with the detection capability of phosphate in potassium dibasic solutions.

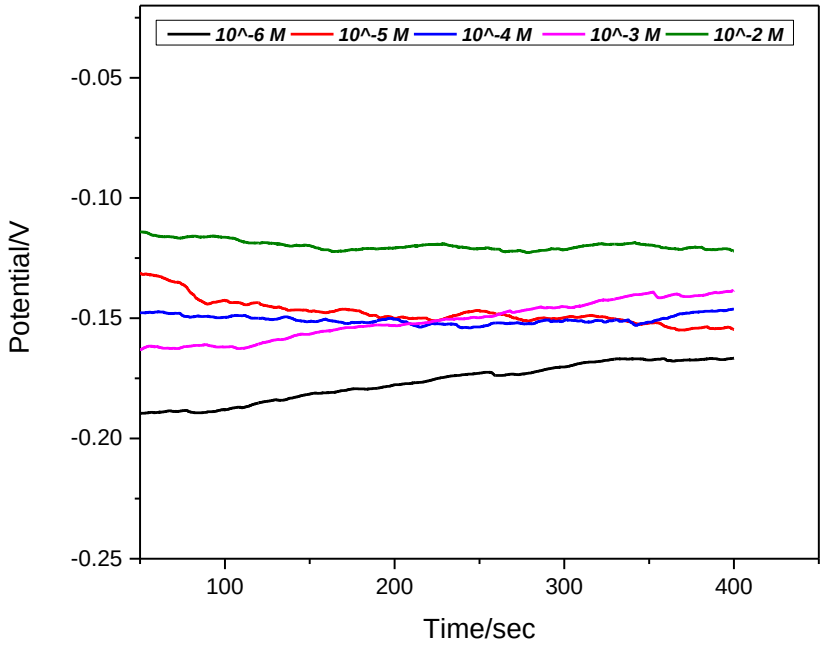

Figure 35: Raw Data Analysis of phosphate detection using K_2HPO_4 Standard Solution (with a range from 10^{-6} to 10^{-2} (mol/L))

Figure 35 is the unrefined data generated with the screen-printed electrode. Low level of fluctuations was noticed throughout the test for each of the solutions. For all of the concentrations, the sensor has showcased enhanced performance in respect to detectivity.

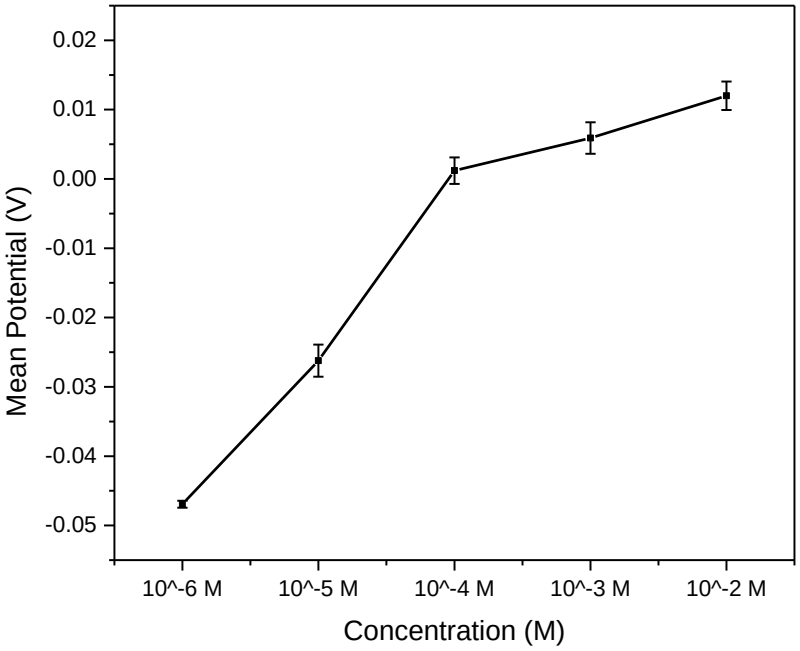

Figure 36: Statistical Analysis of phosphate detection using K_2HPO_4 Standard Solution (with a range from 10^{-6} to 10^{-2} (mol/L))

The standard deviation limit was within ±0.001 to ±0.002 for all the concentrations. The first concentration 10^{-6} (mol/L) and the fourth concentration 10^{-3} (mol/L) has more aberration in signal among the others. But after computing the average values, it can be affirmed that like the other standard solutions of phosphate, the sensor has good capability of detecting phosphate in K_2HPO_4 solutions. As, the potential response is in line with the rise of the phosphate concentrations.

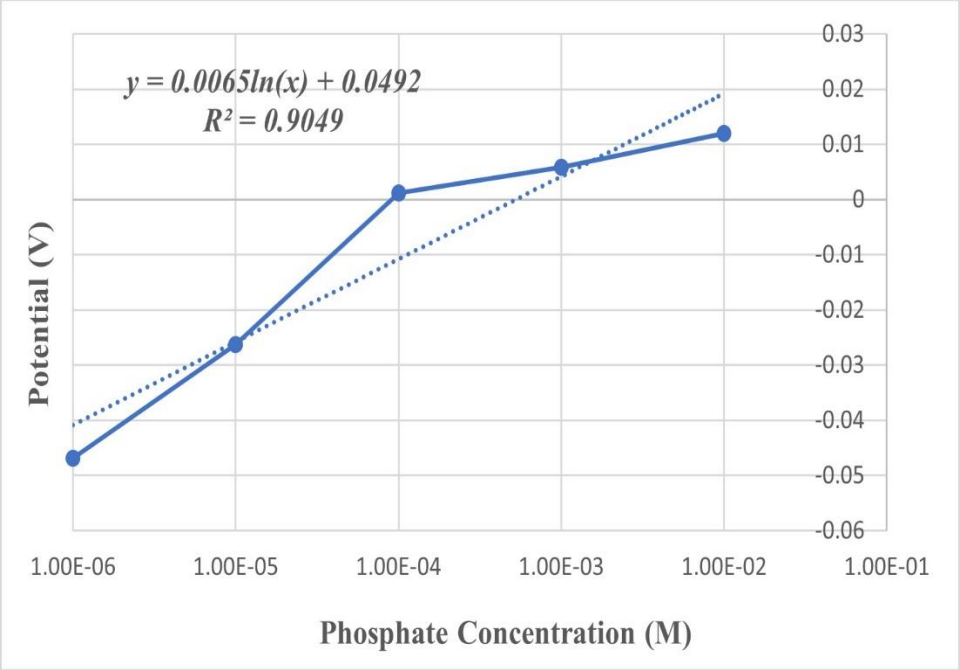

Figure 37: Linear Regression of phosphate detection using K_2HPO_4 Standard Solution (with a range from 10^{-6} to 10^{-2}(mol/L))

Figure 37 is the plot of linear regression plotting Potential (V) Vs. Phosphate Concentration (M) graph. A R^2 value of 0.9049 clearly indicates the potentiality of the sensor in terms of sensing the phosphate in the aqueous solutions.

4.4 Importance of PH in electrochemical detection of phosphate ions

The pH of a solution is a crucial parameter that represents its chemical conditions. The pH can influence nutritional availability, biological functioning, microbial activity, and chemical behavior. As a result, a wide range of applications rely on monitoring or managing the pH of soil, water, and food or beverage items.

Fish and other aquatic life can be affected by water that has a pH that is too low or too high. Poisonous metals like aluminum can enter the water in higher concentrations at low pH, some nitrogen-bearing compounds become more toxic, and fish metabolic processes can become inefficient. Young fish and other aquatic species are especially vulnerable to water with a pH below 5, which can limit reproduction or cause death. Growth can be impeded by water with a pH below 6.5.

The pH is adjusted in wastewater treatment (e.g., sewage or industrial waste) to ensure that desirable chemical or microbiological reactions occur as quickly as feasible. To respond to changing chemical or microbiological conditions, operators carefully monitor and modify the pH.

The development of insoluble calcium phosphate species is caused by high pH levels. The study also revealed the role of organic matter and alkaline phosphate ions in retaining free phosphate ions in solution at high pH levels. However, for maximum availability and uptake by plants, pH in aquaponics systems should be kept in the 5.5–7.2 range [80].

4.5 Open circuit voltammetry analysis with Sodium Phosphate Buffer Solutions

To determine the efficacy of the electrochemical sensors for detecting phosphate in water solutions, we have taken different buffer solutions. Using both NaH_2PO_4 and Na_2HPO_4, the buffer solutions were made. As pH is an important factor in electrochemical sensing, different criteria were used to prove its significance.

4.5.1 Criteria 1: Same Concentration, Different pH

As pH in aqueous solutions should have a limit within the 5.8-7.5 range, in this experiment different pH value-based solutions were made. Using the pH meter, the pH was controlled, and the concentration was kept same which is 10^{-2}(mol/L) to see the effect. A single screen-printed electrode was used to conduct the test. Gradually the pH was increased with keeping the concentration same. The sensor was first dipped into the pH solution of 6 with the concentration 10^{-2}(mol/L). And then with different pH value-based concentrations, the same sensor was used repeatedly. In between each of the experiment, the sensor was washed with DI water to elude any unwanted particles.

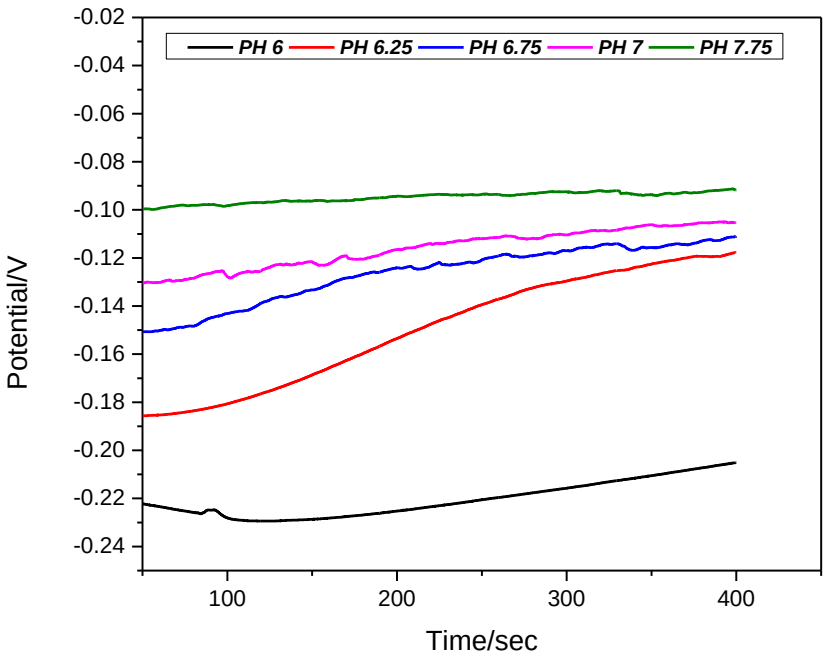

Figure 38: Raw Data Analysis of phosphate detection using Sodium Phosphate Buffer Solution (with a range from pH 6-7.75)

Figure 38 demonstrates the effect of pH in phosphate detection when the concentration is kept same. As, the upper limit of our sensor's phosphate detection is 10^{-2}(mol/L), the concentration was maintained as same as this upper limit with varying the pH value. The potential response has gradually increased with the increment of pH values. None of the curve is overlapped with each other.

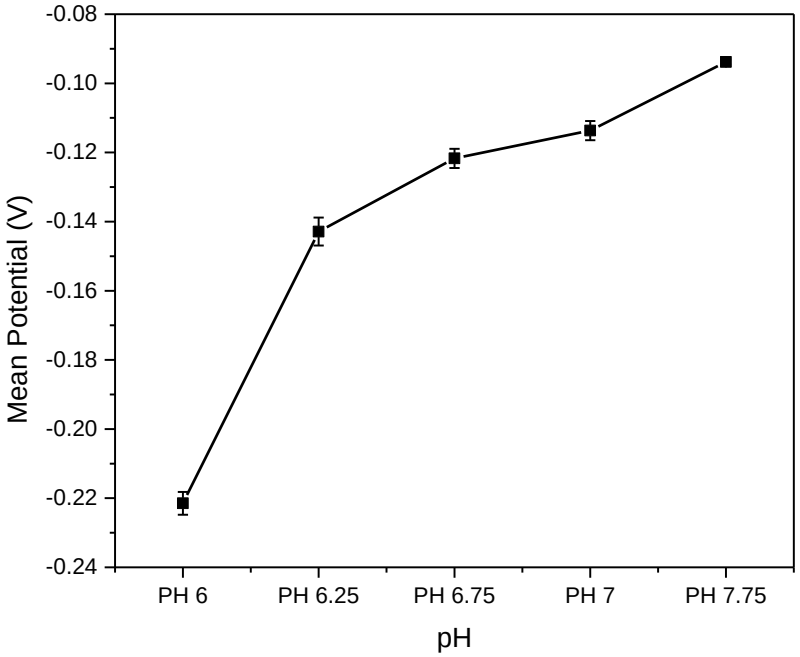

Figure 39: Statistical Data Analysis of phosphate detection using Sodium Phosphate Buffer Solution (with a range from pH 6-7.75)

Figure 39 sums up the mean average value taken within 180-300 seconds of the open-circuit voltammetry analysis. It is clearly seen that, with increasing pH, the potentiality is also increasing. The highest deviation is seen for pH 6.25 and it is ±0.00406.

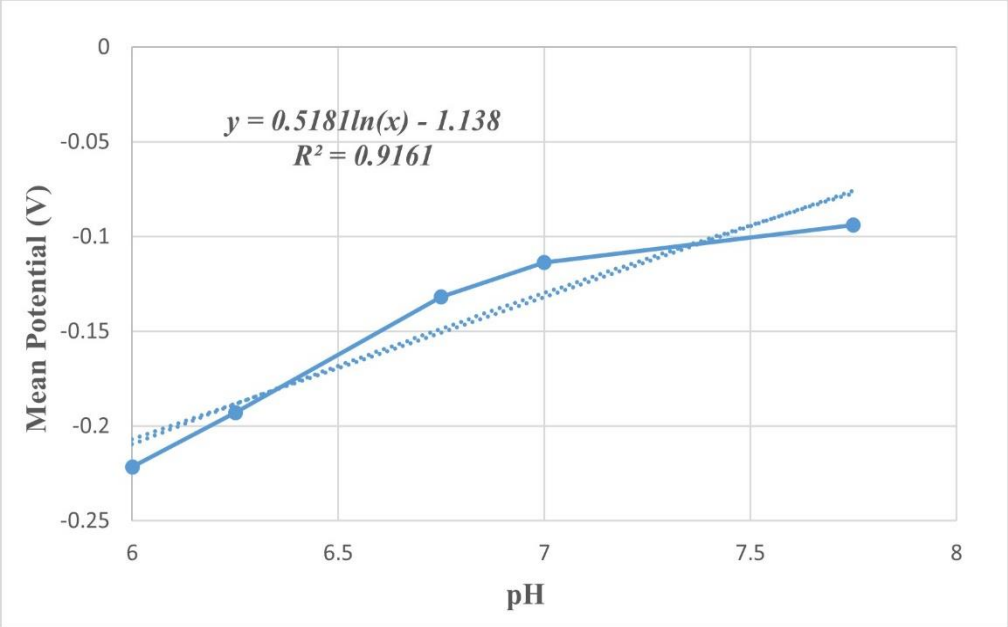

Figure 40: Linear Regression Analysis of phosphate detection using Sodium Phosphate Buffer Solution (with a range from pH 6-7.75)

With a R^2 value of 0.9161, the sensor's effectivity can be manifested in terms of pH change. With same concentration, changing the pH value can create new changes in potential values. The increment in potential response is in proportion with the increase in pH value.

4.5.2 Criteria 2: Same pH, Different Concentrations

Another, criteria have been selected to experiment the effect of pH on our proposed sensor's detection capability. Couple of higher concentrated sodium buffer solutions were tested maintaining fixed pH value like pH-6.5 and pH-7.5.

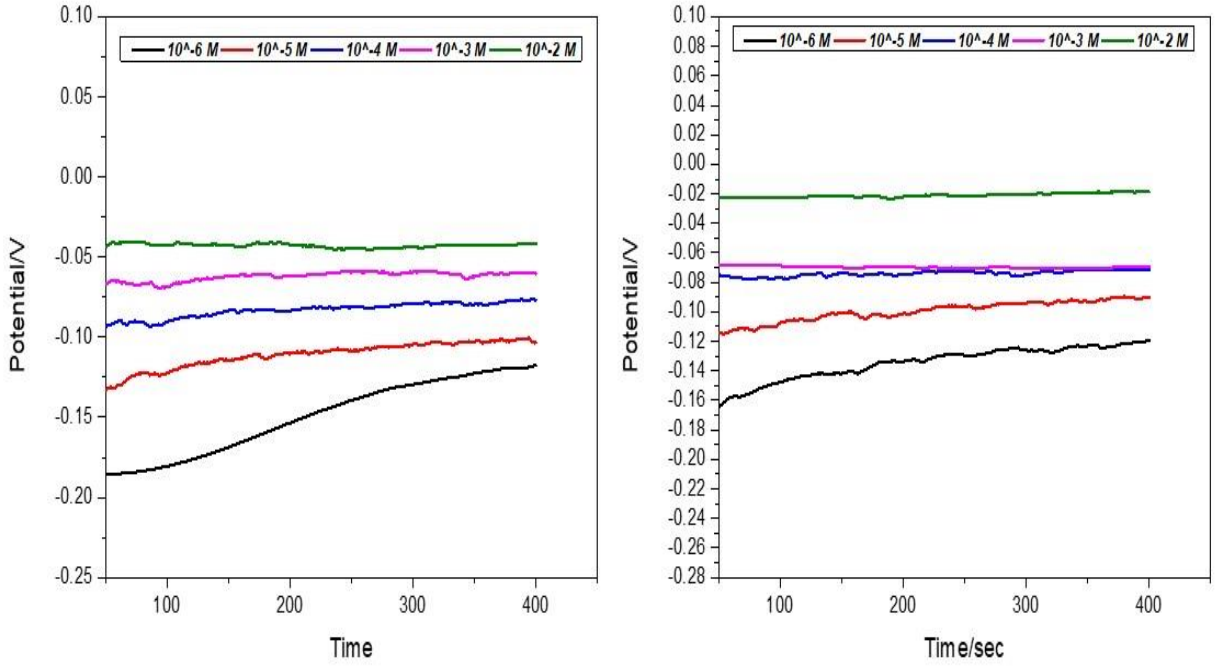

Figure 41: Raw Data Analysis of phosphate detection using Sodium Phosphate Buffer Solution: pH 6.5 (left) and pH 7.5 (right)

From Figure 41, it can be predicted that whether the pH value is different, for both experiment the potentiality of the phosphate concentrations has similar range. For 10^{-6} to 10^{-2} (mol/L) range of concentration, the potential lies in between -0.02V to -0.2V range. And different pH value of 6.5 and 7.5 did not affect the potential response.

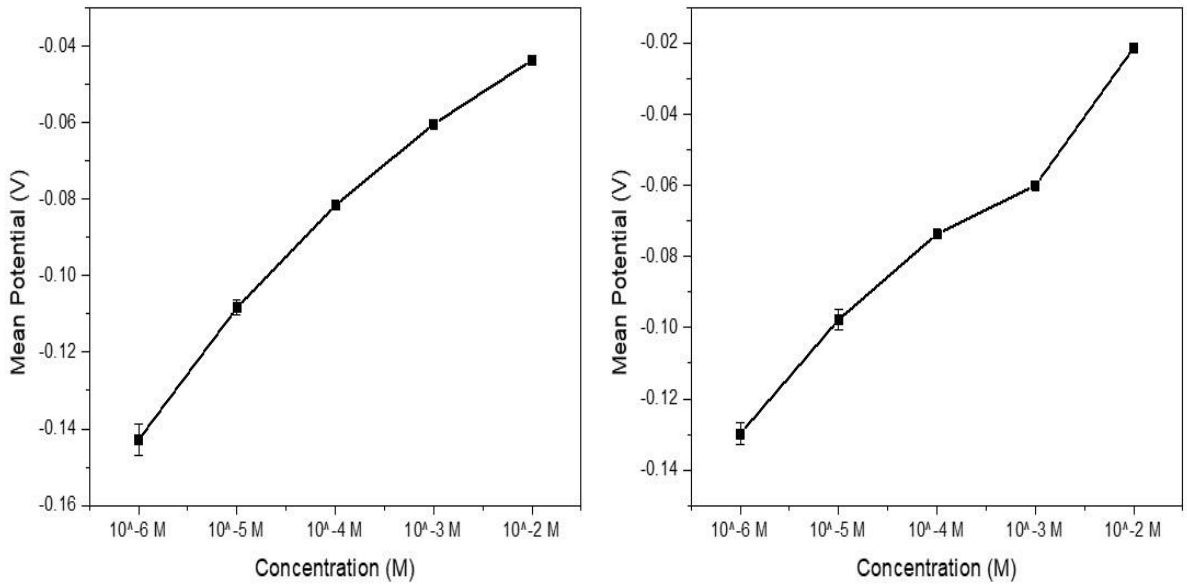

Figure 42: Statistical Data Analysis of phosphate detection using Sodium Phosphate Buffer Solution: pH 6.5 (left) and pH 7.5 (right)

Same as before, the mean value for all the concentration in both pH experiment, lies in between -0.02V to -0.15V range. The two individual sensors that were used for the experiments, have experienced a fluctuation at the starting. The deviation range was within ±0.004 to ±0.003 for the 10^{-6} (mol/L). It is expected as the sensor takes some seconds to get adjusted with the solution environment.

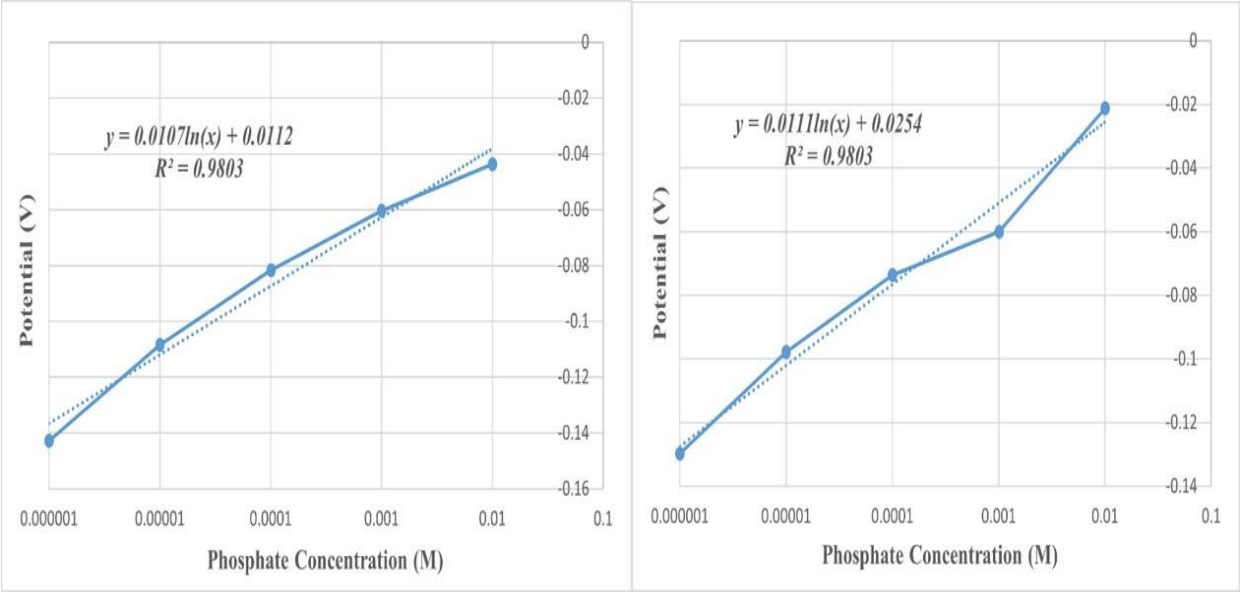

Figure 43: Linear Regression Analysis of phosphate detection using Sodium Phosphate Buffer Solution: pH 6.5 (left) and pH 7.5 (right)

Though the characteristic curve for pH 6.5 and pH 7.5 is different from each other, the R^2 value is same, and it is 0.9803. It strongly proves that whether there is change in pH if the concentration is same then the potential response should be in close range for any of the sensors.

4.6 Open circuit voltammetry analysis with Potassium Phosphate Buffer Solutions

To determine the efficacy of the electrochemical sensors for detecting phosphate in water solutions, we have taken different buffer solutions. KH_2PO_4 and K_2HPO_4 were used to make the potassium phosphate buffer solutions. With maintaining different values of pH, the test was done.

4.6.1 Criteria 1: Same Concentration, Different pH

Because pH in aqueous solutions should be kept within the range of 5.8-7.5, multiple pH value-based solutions were created in this experiment. The pH was adjusted with a pH meter, and the concentration was kept constant at 10^{-2}(mol/L) to see the effect. The test was carried out with a single screen-printed electrode. The pH was gradually raised while the concentration remained constant. First, the sensor was immersed in a pH solution of 6 with a concentration of 10^{-2}(mol/L). The same sensor was then utilized repeatedly with varying pH value-based concentrations. The sensor was rinsed with DI water in between each experiment to remove any undesirable particles.

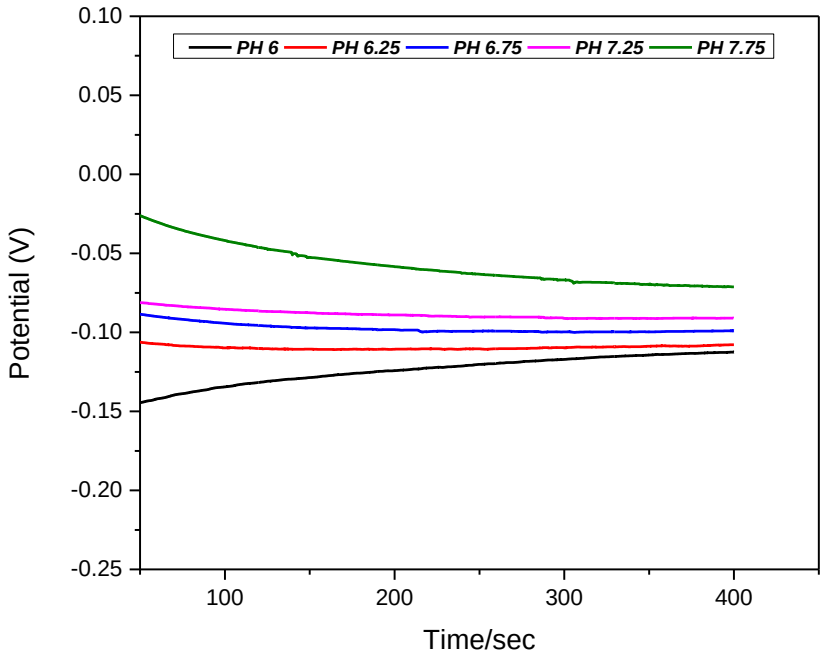

Figure 44: Raw Data Analysis of phosphate detection using Potassium Phosphate Buffer Solution (with a range from pH 6-7.75)

When the concentration is kept constant, Figure 44 shows the influence of pH on phosphate detection. Because the highest limit of our sensor's phosphate detection is 10^{-2}(mol/L), the concentration was kept constant while the pH was varied. With increasing pH values, the potential response has gradually grown. There is no crossover between any of the curves.

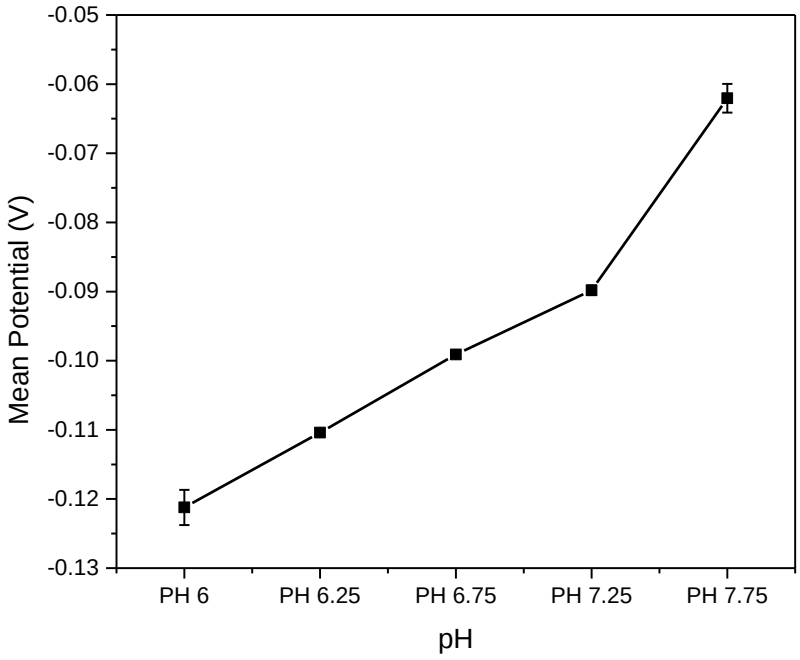

Figure 45: Statistical Data Analysis of phosphate detection using Potassium Phosphate Buffer Solution (with a range from pH 6-7.75)

The mean average value taken within 180-300 seconds of the open-circuit voltammetry analysis is summarized in Figure 38. It can readily be seen that as the pH rises, so does the potentiality. pH 6 has the largest variation, which is 0.00231.

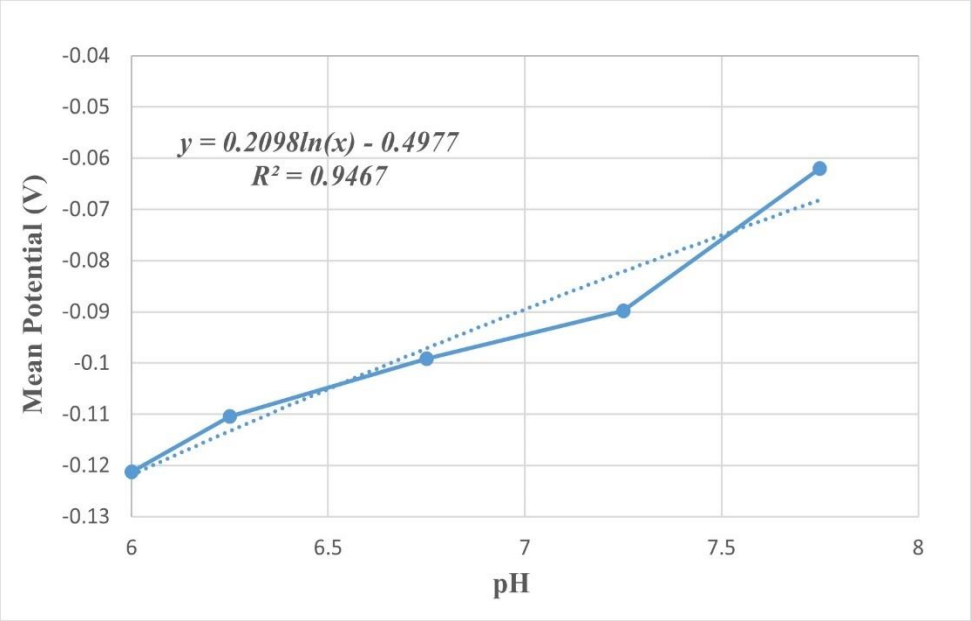

Figure 46: Linear Regression Analysis of phosphate detection using Potassium Phosphate Buffer Solution (with a range from pH 6-7.75)

The sensor's effectivity can be measured in terms of pH change, according to an R^2 value of 0.9467. Changing the pH value while maintaining the same concentration can result in fresh variations in potential values. The increase in potential response is proportional to the rise in pH level.

4.6.2 Criteria 2: Same pH, Different Concentrations

Same as the sodium phosphate buffer solutions, the potassium phosphate buffer solutions were also experimented for same pH, different concentrations. With a range of 10^{-6} to 10^{-2} (mol/L) concentrated solutions, the test was done using fixed pH value like pH-6.5 and pH-7.5.

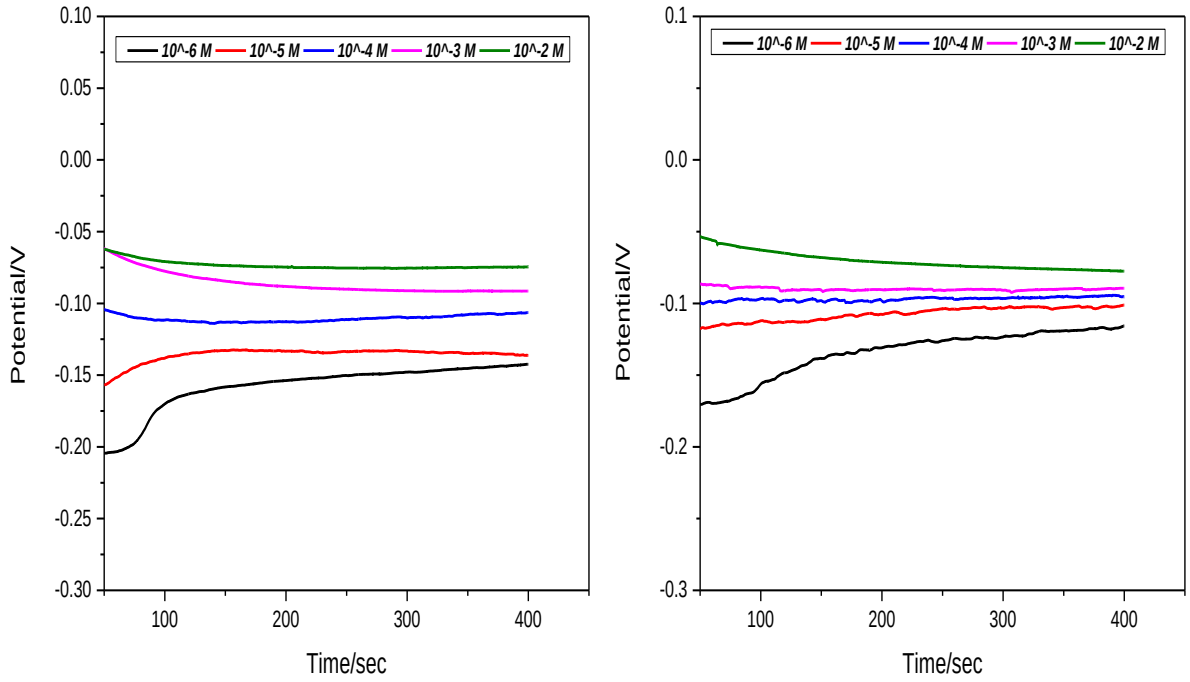

Figure 47: Raw Data Analysis of phosphate detection using Potassium Phosphate Buffer Solution: pH 6.5 (left) and pH 7.5 (right)

Figure 47 shows that, regardless of the pH value, the potentiality of the phosphate concentrations in both experiments has a comparable range. The potential is between -0.05V and -0.2V for concentrations ranging from 10^{-6} to 10^{-2} (mol/L). The potential response was unaffected by pH values of 6.5 and 7.5.

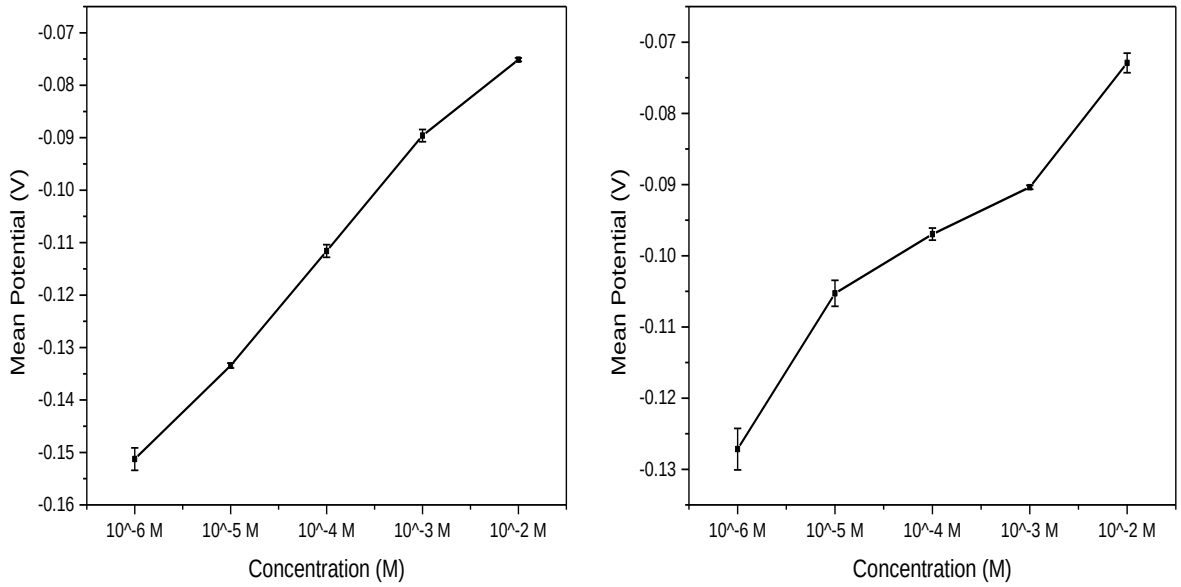

Figure 48: Statistical Data Analysis of phosphate detection using Potassium Phosphate Buffer Solution: pH 6.5 (left) and pH 7.5 (right)

Similarly, like the previous experiment, the mean value for all concentrations in both pH experiments is in the -0.07V to -0.15V range. The two individual sensors that were employed in the studies had a fluctuation when they first started. For the 10^{-6} (mol/L), the deviation range was 0.004 to 0.003. It is to be expected, as the sensor adjusts to the solution environment over time.

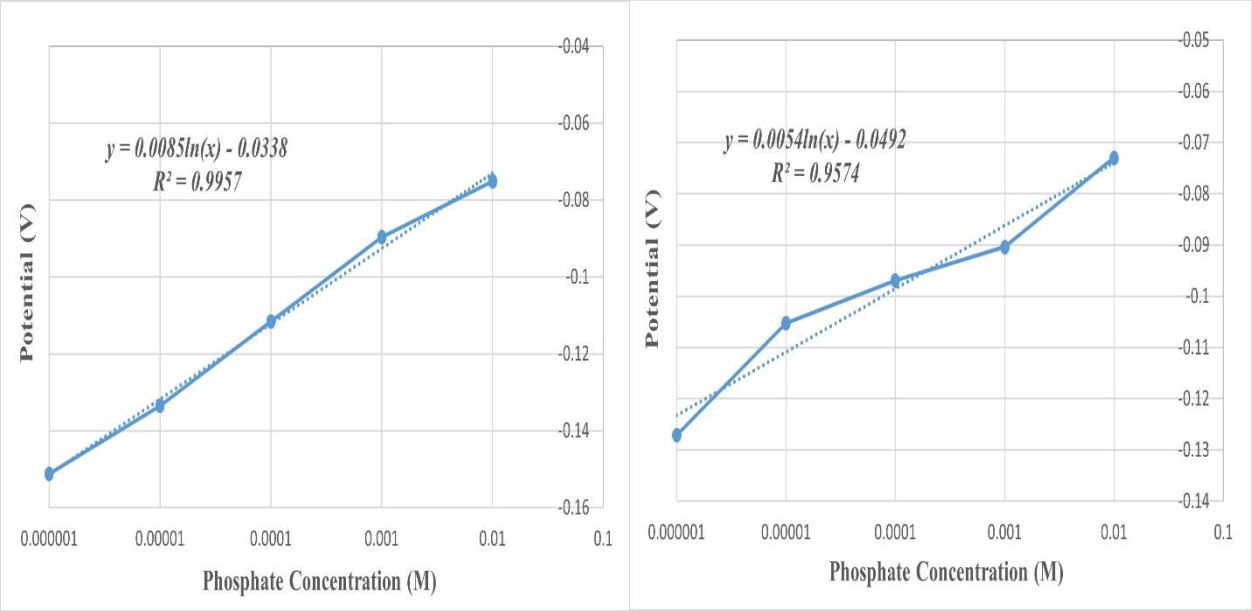

Figure 49: Linear Regression Analysis of phosphate detection using Potassium Phosphate Buffer Solution: pH 6.5 (left) and pH 7.5 (right)

With an excellent R^2 value of 0.9957 (close to ideal 1) for pH 6.5 and 0.9574 for pH 7.5 clearly shows that even if the pH changes, if the concentration remains constant, the potential response for any of the sensors should be within a reasonable range.

4.6 Reproducibility of the proposed sensor

To determine the efficiency of the electrochemical sensors for detecting phosphate in similar fashion, we have taken several sensors and tested with the phosphate solutions. With the concentration range from 10^{-11} to 10^{-2} (mol/L), the sensors were tested to see if all of them have similar potential response and range.

4.6.1 Test with Sodium phosphate solutions

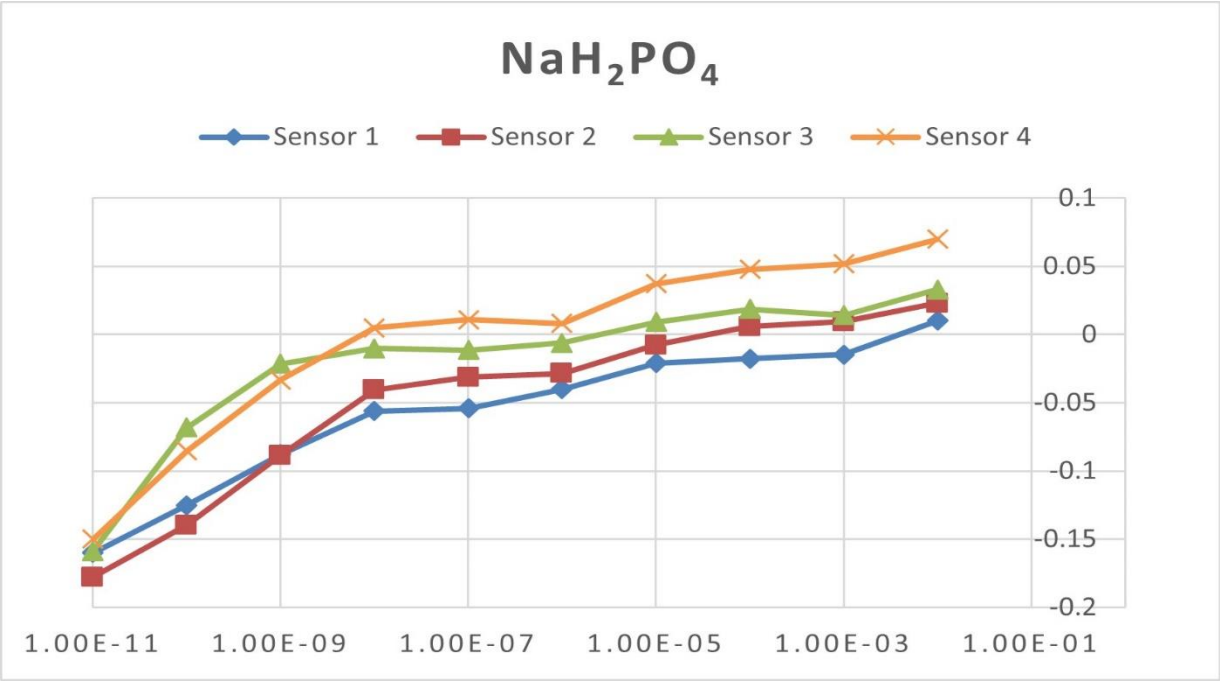

Figure 50: Potential Response for different sensors using NaH_2PO_4 Standard Solution (with a range from 10^{-11} to 10^{-2}(mol/L))

Multiple sensors were tested maintaining the same conditions as the previous experiments to see if the sensors have any variation in detecting phosphate. The above graph is the depiction of 4 individual sensors result with the range from 10^{-11} to 10^{-2} (mol/L). The sensors were washed with deionized water before testing with each of the concentrations.

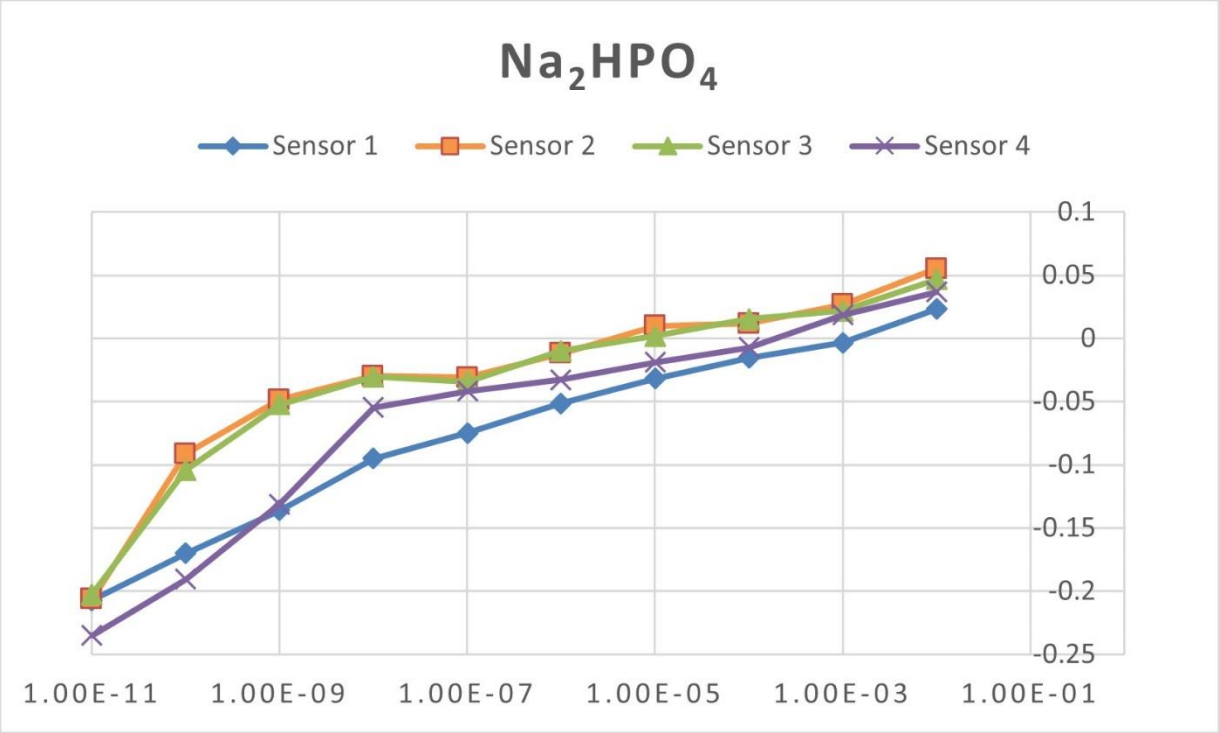

Figure 51: Potential Response for different sensors using Na_2HPO_4 Standard Solution (with a range from 10^{-11} to 10^{-2}(mol/L))

Similarly, for Na_2HPO_4 Standard Solution, couple of sensors were tested to observe the reliability of the proposed sensor. From Figure 51, all of the sensors have similar range and effect in terms of voltage value.

All of the sensors have shown similar characteristics in terms of potential response. It can be easily demonstrated that the sensors have the capability of detecting phosphate with similar effect. For the monobasic and dibasic solutions of sodium phosphate, the potential response for the sensors were in corresponding range.

4.6.2 Test with Potassium phosphate solutions

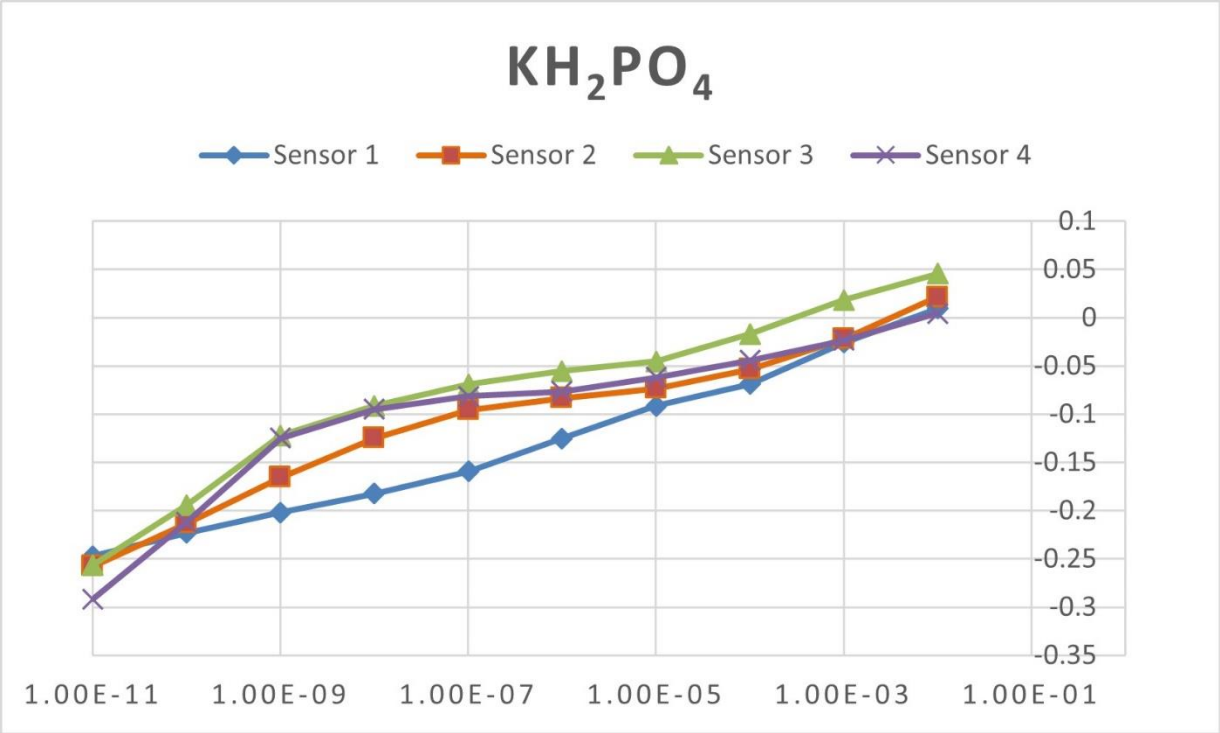

Figure 52: Potential Response for different sensors using KH_2PO_4 Standard Solution (with a range from 10^{-11} to 10^{-2}(mol/L))

Different sensors were tested maintaining the identical state as the previous experiments to see if the sensors have any discrepancy in detecting phosphate. Figure 52 is the representation of 4 separate sensors result that was tested in KH_2PO_4 solution with the range from 10^{-11} to 10^{-2} (mol/L).

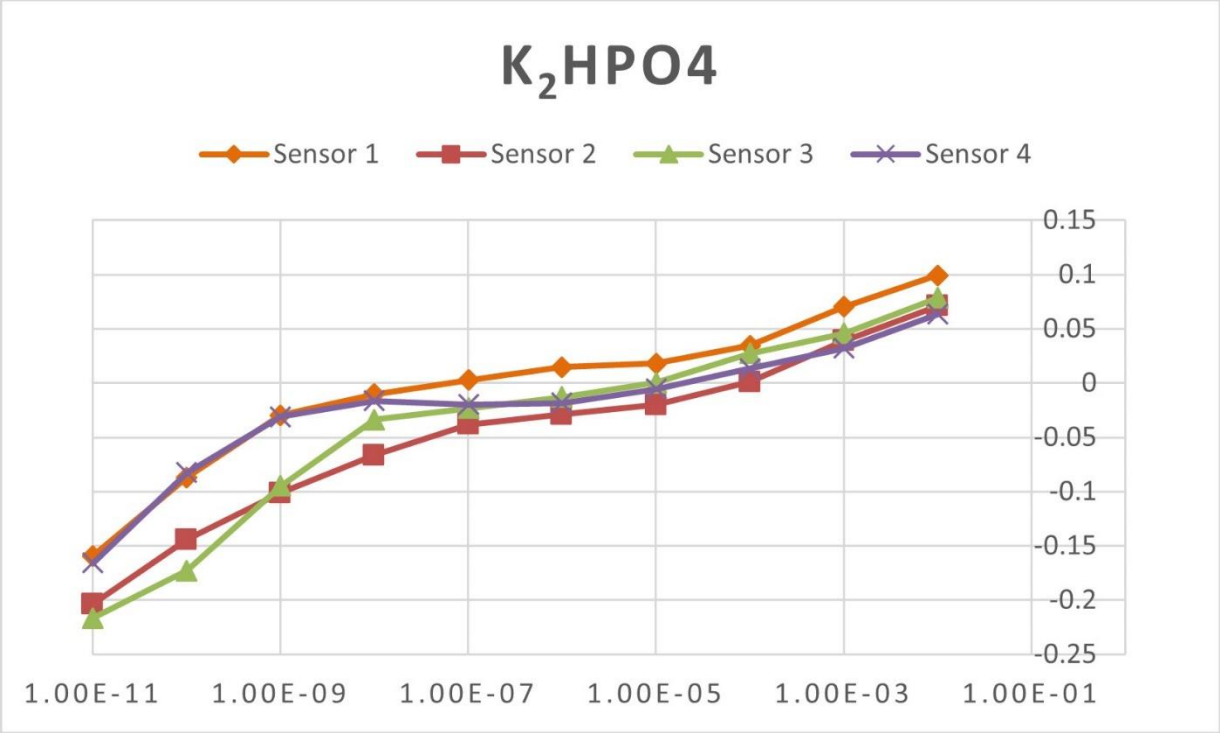

Figure 53: Potential Response for different sensors using K_2HPO_4 Standard Solution (with a range from 10^{-11} to 10^{-2}(mol/L))

Similarly, for K_2HPO_4 Standard Solution, couple of sensors were tested to observe the dependability of the proposed sensor. From Figure 53, all of the sensors have adjacent range and effect in terms of voltage value.

All of the sensors have shown related qualities in terms of potential feedback. It can be illustrated that the sensors have the capability of detecting phosphate within equivalent range . For the monobasic and dibasic solutions of potassium phosphate, the potential response for the sensors were in alike range.

Chapter 5: Conclusion

5.1 Summary and Discussion

The designed sensor has shown promising and good results in terms of lower detection limit and sensitivity for quick in-situ monitoring of phosphate ions in water. With the detection range from 10^{-11} to 10^{-2} (mol/L), the developed sensor has upstanding quality in terms of good fit (logarithmic fit) and applied conditions. With the buffer solutions, maintaining different criteria for pH, the sensor has displayed great character for potential response. The proposed sensor, with its lightweight form and easy mobility, can easily replace the current bulk instruments and methods for detecting phosphate. To detect phosphate levels in aqueous solutions, this sensor, like traditional approaches, does not require expert staff or expensive instruments. As a result, the disposable phosphate sensor based on screen-printed electrodes (SPE) has a lot of potential for cost-effective and on-site examination of water samples.

5.2 Future Work

1. The majority of existing research (such as this one) have only proven water sensor applications that can detect phosphates in standard and buffer solutions. The main challenge in using the developed sensor to detect phosphates in real-world samples (tap water, wastewater, or river water) without changing the pH or other operating conditions is the severe interference of organic-inorganic chemicals and biological constituents in a solution like tap water or wastewater. A pH sensor has been developed in the lab that can measure pH in aqueous solutions. Both the sensors can be integrated together where we can get the pH value at first and then we measure the phosphate concentration.

2. Presently, the electrochemical analyzer (CHI-6012E) that has been used in this research for electrochemical analysis is very expensive. So, the low-cost sensor that has been developed here, needs a device that can have instantaneous potential response in real world sample checking. The best way is to design and integrate a cheap potentiostat for instant data recording. The sensor and the potentiostat will be amalgamated in such a way that it can be used as a handheld device.

3. The available phosphate detectors and instruments in the market are designed only for commercial use. As the price is high, the detectors are irrelevant in terms of domestic usage. So, a cost-effective and transportable sensor unit (with a low cost potentiostat) with having the disposable capability can be high yielding for both commercials and households.

References

[1] G. Kongshaug *et al.*, "Phosphate Fertilizers," in *Ullmann's Encyclopedia of Industrial Chemistry*, Weinheim, Germany: Wiley-VCH Verlag GmbH & Co. KGaA, 2014, pp. 1–49.

[2] US EPA, "Nutrient Pollution: The Environmental Problem." [Online]. Available: https://www.epa.gov/nutrientpollution/problem. [Accessed: 24-Dec-2020].

[3] A. M. Michalak *et al.*, "Record-setting algal bloom in Lake Erie caused by agricultural and meteorological trends consistent with expected future conditions," *Proc. Natl. Acad. Sci.*, vol. 110, no. 16, pp. 6448–6452, Apr. 2013.

[4] "NOAA, partners predict significant harmful algal bloom in western Lake Erie this summer."[Online].Available: http://www.noaanews.noaa.gov/stories2014/20140710_erie_hab.html. [Accessed: 24-Dec-2020].

[5] "Phosphate : Its Importance in Water and Its Measurement," pp. 3–7.

[6] B. Gordon, P. Callan, and C. Vickers, "WHO guidelines for drinking-water quality.," *WHO Chron.*, vol. 38, no. 3, p. 564, 2008.

[7] US EPA, "Why do water systems add phosphate to drinking water? What are the health effects of drinking water containing phosphates. – Ground Water & Drinking Water." [Online]. Available: https://safewater.zendesk.com/hc/en-us/articles/211406008-Why-do-water-systems-add-phosphate-to-drinking-water-What-are-the-health-effects-of-drinking-water-containing-phosphates-. [Accessed: 24-Dec-2020].

[8] NSF/ANSI, "Drinking Water Treatment Chemicals - Health Effects," 2013.

[9] B. A. Bpa, "NSF International," p. 84120, 2007.

[10] Howard Perlman, "Phosphorus and water: The USGS Water Science School," *U.S. Geological Survey*. [Online]. Available: https://water.usgs.gov/edu/phosphorus.html. [Accessed: 25-Dec-2020].

[11] D. Hem, "Study and Interpretation the Chemical Characteristics of Natural Water," *USGS*, vol. 2254, no. 2254, p. 263, 1985.

[12] Department of Natural Resources, "Chapter NR 217: effluent standards and limitations for phosphorus," *Effl. Stand. Limitations*, no. 217, p. 8 pp., 2013.

[13] Department of Natural Resources, "WATER QUALITY STANDARDS FOR WISCONSIN SURFACE WATERS," *Effl. Stand. Limitations*.

[14] "Water Resource Characterization DSS - Phosphorus." [Online]. Available: http://www.water.ncsu.edu/watershedss/info/phos.html. [Accessed: 25-Dec-2017].

[15] J. E. Kotoski, "Phosphorus Analysis Sheet: Information on Phosphorus Amounts, Water Quality," *Spring Harb. Environ. Magn. Middle Sch.*, 1997.

[16] W.-L. Cheng, J.-L. Chang, Y.-L. Su, and J.-M. Zen, "Facile Fabrication of Zirconia Modified Screen-Printed Carbon Electrodes for Electrochemical Sensing of Phosphate," *Electroanalysis*, vol. 25, no. 12, pp. 2605–2612, 2013.

[17] S. Berchmans, T. B. Issa, and P. Singh, "Determination of inorganic phosphate by electroanalytical methods: A review," *Anal. Chim. Acta*, vol. 729, pp. 7–20, 2012.

[18] N. Nakatani *et al.*, "Simultaneous spectrophotometric determination of phosphate and silicate ions in river water by using ion-exclusion chromatographic separation and post-column derivatization," *Anal. Chim. Acta*, vol. 619, no. 1, pp. 110–114, 2008.

[19] A. Duerkop, M. Turel, A. Lobnik, and O. S. Wolfbeis, "Microtiter plate assay for phosphate using a europium–tetracycline complex as a sensitive luminescent probe," *Anal. Chim. Acta*, vol. 555, pp. 292–298, 2006.

[20] X. Lin, X. Wu, Z. Xie, and K.-Y. Wong, "PVC matrix membrane sensor for fluorescent determination of phosphate," *Talanta*, vol. 70, no. 1, pp. 32–36, Aug. 2006.

[21] M. J. Vazquez, B. Rodriguez, C. Zapatero, and D. G. Tew, "Determination of phosphate in nanomolar range by an enzyme-coupling fluorescent method," *Anal. Biochem.*, vol. 320, no. 2, pp. 292–298, Sep. 2003.

[22] R. N. Fernandes and B. F. Reis, "Flow system exploiting multicommutation to increase sample residence time for improved sensitivity. Simultaneous determination of ammonium and ortho-phosphate in natural water," *Talanta*, vol. 58, no. 4, pp. 729–737, Oct. 2002.

[23] P. . Antony, S. Karthikeyan, and C. S. . Iyer, "Ion chromatographic separation and determination of phosphate and arsenate in water and hair," *J. Chromatogr. B*, vol. 767, no. 2, pp. 363–368, Feb. 2002.

[24] M. M. G. Antonisse and D. N. Reinhoudt, "Potentiometric Anion Selective Sensors," *Electroanalysis*, vol. 11, no. 14, pp. 1035–1048, Oct. 1999.

[25] P. Fossati, "Phosphate determination by enzymatic colorimetric assay," *Anal. Biochem.*, vol. 149, no. 1, pp. 62–65, Aug. 1985.

[26] I. Debruyne, "Inorganic phosphate determination: Colorimetric assay based on the formation of a rhodamine B-phosphomolybdate complex," *Anal. Biochem.*, vol. 130, no. 2, pp. 454–460, Apr. 1983.

[27] E. Climent, R. Casasús, M. D. Marcos, R. Martínez-Máñez, F. Sancenón, and J. Soto, "Colorimetric sensing of pyrophosphate in aqueous media using bis-functionalised silica surfaces," *Dalt. Trans.*, vol. 0, no. 24, p. 4806, Jun. 2009.

[28] I. A. Azath, P. Suresh, and K. Pitchumani, "Per-6-ammonium-β-cyclodextrin/p-nitrophenol complex as a colorimetric sensor for phosphate and pyrophosphate anions in water," *Sensors Actuators B Chem.*, vol. 155, no. 2, pp. 909–914, Jul. 2011.

[29] "AFFINITY CHROMATOGRAPHY," *Publ. by InTech Janeza Trdine*, vol. 9, 5100.

[30] M. A. Bello and A. G. Gonzalez, "Determination of Phosphate in Cola Beverages Using Nonsuppressed Ion Chromatography: An Experiment Introducing Ion Chromatography for Quantitative Analysis," *J. Chem. Educ.*, vol. 73, no. 12, p. 1174, Dec. 1996.

[31] M. Colina, H. Ledo, E. Gutiérrez, E. Villalobos, and J. Marín, "Determination of total phosphorus in sediments by means of high-pressure bombs and ion chromatography," *J. Chromatogr. A*, vol. 739, no. 1–2, pp. 223–227, Jul. 1996.

[32] H. L. de Medina, E. Gutiérrez, M. C. de Vargas, G. González, J. Marín, and E. Andueza,

"Determination of phosphate and sulphite in natural waters in the presence of high sulphate concentrations by ion chromatography under isocratic conditions," *J. Chromatogr. A*, vol. 739, no. 1–2, pp. 207–215, Jul. 1996.

[33] R. De Marco and C. Phan, "Determination of phosphate in hydroponic nutrient solutions using flow injection potentiometry and a cobalt-wire phosphate ion-selective electrode.," *Talanta*, vol. 60, no. 6, pp. 1215–21, Aug. 2003.

[34] M. C. T. Diniz, O. F. Filho, E. V. de Aquino, and J. J. R. Rohwedder, "Determination of phosphate in natural water employing a monosegmented flow system with simultaneous multiple injection," *Talanta*, vol. 62, no. 3, pp. 469–475, Feb. 2004.

[35] K.-H. Chen, J.-H. Liao, H.-Y. Chan, and J.-M. Fang, "A Fluorescence Sensor for Detection of Geranyl Pyrophosphate by the Chemo-Ensemble Method," *J. Org. Chem.*, vol. 74, no. 2, pp. 895–898, Jan. 2009.

[36] A. N. Ejhieh and N. Masoudipour, "Application of a new potentiometric method for determination of phosphate based on a surfactant-modified zeolite carbon-paste electrode (SMZ-CPE)," *Anal. Chim. Acta*, vol. 658, no. 1, pp. 68–74, Jan. 2010.

[37] S. Cosnier *et al.*, "A glucose biosensor based on enzyme entrapment within polypyrrole films electrodeposited on mesoporous titanium dioxide," *J. Electroanal. Chem.*, vol. 469, no. 2, pp. 176–181, Jul. 1999.

[38] A. O. Scott, "Biosensors for Food Analysis."

[39] Wah On Ho *et al.*, "Electrochemical Sensor for Measurement of Urea and Creatinine in Serum Based on ac Impedance Measurement of Enzyme-Catalyzed Polymer Transformation," 1999.

[40] L. Song, L. Zhu, Y. Liu, X. Zhou, and H. Shi, "A disposable cobalt-based phosphate sensor based on screen printing technology," *Sci. China Chem.*, vol. 57, no. 9, pp. 1283–1290, 2014.

[41] J. Chang, G. Zhou, E. R. Christensen, R. Heideman, and J. Chen, "Graphene-based sensors for detection of heavy metals in water: a review," *Anal. Bioanal. Chem.*, vol. 406, no. 16, pp. 3957–3975, 2014.

[42] R. Seenivasan, W.-J. Chang, and S. Gunasekaran, "Highly Sensitive Detection and Removal of Lead Ions in Water Using Cysteine-Functionalized Graphene Oxide/Polypyrrole Nanocomposite Film Electrode-Supporting Document," *Evolution (N. Y).*, pp. 1224–1227, 2015.

[43] M. Li, Y. Li, D. Li, and Y. Long, "Recent developments and applications of screen-printed electrodes in environmental assays — A review," *Anal. Chim. Acta*, vol. 734, pp. 31–44, 2012.

[44] P. FANJULBOLADO, P. QUEIPO, P. LAMASARDISANA, and A. COSTAGARCIA, "Manufacture and evaluation of carbon nanotube modified screen-printed electrodes as electrochemical tools," *Talanta*, vol. 74, no. 3, pp. 427–433, Dec. 2007.

[45] N. Thiyagarajan, J. L. Chang, K. Senthilkumar, and J. M. Zen, "Disposable electrochemical sensors: A mini review," *Electrochem. commun.*, vol. 38, pp. 86–90, 2014.

[46] “Hanna Checkers® Handheld Phosphate Colorimeters - Hanna Instruments.” [Online]. Available:https://hannainst.com/products/checker colorimeters.html#filter:parameter:Phosphate. [Accessed: 24-Dec-2020].

[47] “HANNA® Ion Specific Meters | Ben Meadows.” [Online]. Available: https://www.benmeadows.com/hanna-ion-specific-meters_36816675. [Accessed: 27-Dec-2020].

[48] “Hach 5870006 Pocket Colorimeter Ii, Phosphate, O- from Cole-Parmer.” [Online]. Available:https://www.coleparmer.com/i/hach-5870006-pocket-colorimeter-ii-phosphate-. [Accessed: 27-Dec-2020].

[49] “PHOSPHAX sc Phosphate Analyzer, 1-50mg/l PO4-P, 115V, 5m Filter Probe sc | Hach USA - Overview.” [Online]. Available: https://www.hach.com/phosphax-sc-phosphate-analyzer-1-50mg-l-po4-p-115v-5m-filter-probe-sc/product?id=7640094094&. [Accessed: 27-Dec-2020].

[50] † Akio Ojida, † Yasuko Mito-oka, † and Kazuki Sada, and †,‡,§ Itaru Hamachi*, “Molecular Recognition and Fluorescence Sensing of Monophosphorylated Peptides in Aqueous Solution by Bis(zinc(II)−dipicolylamine)-Based Artificial Receptors,” 2004.

[51] † Akio Ojida, † Yasuko Mito-oka, † and Masa-aki Inoue, and †,‡,§ Itaru Hamachi*, “First Artificial Receptors and Chemosensors toward Phosphorylated Peptide in Aqueous Solution,” 2002.

[52] B. Zhang and H. P. Beck, “A RAPID AND SENSITIVE METHOD FOR THE FLUORIMETRIC DETERMINATION OF PHOSPHATE BY FLOW-INJECTION,” *Anal. Lett.*, vol. 34, no. 15, pp. 2721–2733, Dec. 2001.

[53] R. K. M. and and M. E. Meyerhoff*, “Mixed Potential Response Mechanism of Cobalt Electrodes toward Inorganic Phosphate,” 1996.

[54] W. H. Lee, Y. Seo, and P. L. Bishop, “Characteristics of a cobalt-based phosphate microelectrode for in situ monitoring of phosphate and its biological application.,” *Sens. Actuators. B. Chem.*, vol. 137, no. 1, pp. 121–128, Mar. 2009.

[55] S. Cinti, D. Neagu, M. Carbone, I. Cacciotti, D. Moscone, and F. Arduini, “Novel carbon black-cobalt phthalocyanine nanocomposite as sensing platform to detect organophosphorus pollutants at screen-printed electrode,” *Electrochim. Acta*, vol. 188, pp. 574–581, 2016.

[56] “Phosphate Detection,” Jul. 2012.

[57] R. Gächter*, J. M. Ngatiah†, and C. Stamm, “Transport of Phosphate from Soil to Surface Waters by Preferential Flow,” 1998.

[58] R. Gilmore, “Laboratory Studies in Chemically Mediated Phosphorus Removal,” *Theses Diss.*, Jan. 2009.

[59] B. N. Horwitt, “Determeination of inorganic serum phosphate by means of stannous chloride,” *Dep. Med. Tulane Univ. Med. Endocr. Res. Lab. Allon Ochsner Med. Found. New Orleans, Lousiana*, no. June 1952, pp. 1–10, 1952.

[60] A. Henriksen, “Application of a modified stannous chloride reagent for determining

orthophosphate," *Analyst*, vol. 88, no. 1052, p. 898, Jan. 1963.

[61] "Stannous Chloride Reagent II, for Phosphate Analysis (with extraction)." [Online]. Available:https://www.fishersci.com/shop/products/stannous-chloride-reagent-ii-phosphate-analysis-with-extraction-ricca-chemical-3/799816. [Accessed: 31-Mar-2021].

[62] W. A. Cilley, "Solubility of tin(II) orthophosphate and the phosphate complexes of tin(II)," *Inorg. Chem.*, vol. 7, no. 3, pp. 612–614, Mar. 1968.

[63] O. Sletten and C. M. Bach, "Modified Stannous Chloride Reagent for Orthophosphate Determination," *Journal (American Water Works Association)*, vol. 53. American Water Works Association, pp. 1031–1033, 1961.

[64] A. T. Law Al and S. B. Adeloju, "Progress and recent advances in phosphate sensors: A review," *Talanta*, vol. 114, pp. 191–203, 2013.

[65] A. C. Javier, S. R. Crouch, and H. V. Malmstadt, "Investigations of formation of 12-molybdophosphoric acid utilizing rapid reaction-rate measurements," *Anal. Chem.*, vol. 40, no. 13, pp. 1922–1925, Nov. 1968.

[66] D. Talarico, S. Cinti, F. Arduini, A. Amine, D. Moscone, and G. Palleschi, "Phosphate Detection through a Cost-Effective Carbon Black Nanoparticle-Modified Screen-Printed Electrode Embedded in a Continuous Flow System," *Environ. Sci. Technol.*, vol. 49, no. 13, pp. 7934–7939, 2015.

[67] "Open Circuit Potential (OCP)," Pineresearch.com, 06-Mar-2019. [Online]. Available: https://pineresearch.com/shop/kb/software/methods-and-techniques/basic-methods/open-circuit-potential-ocp/. [Accessed: 05-Jun-2021].

[68] H. A. Videla, Manual of Biocorrosion. Boca Raton, FL: CRC Press, 1996.

[69] P. W. Baker, K. Ito, and K. Watanabe, "Marine prosthecate bacteria involved in the ennoblement of stainless steel," Environ. Microbiol., vol. 5, no. 10, pp. 925–932, 2003.

[70] J. Dumańska and K. Maksymiuk, "Studies on spontaneous charging/discharging processes of polypyrrole in aqueous electrolyte solutions," Electroanalysis, vol. 13, no. 7, pp. 567–573, 2001.

[71] Y. Song, D. Su, Y. Shen, H. Liu, and L. Wang, "Design and preparation of open circuit potential biosensor for in vitro and in vivo glucose monitoring," Anal. Bioanal. Chem., vol. 409, no. 1, pp. 161–168, 2017.

[72] A. P. R. Souza, C. W. Foster, A. V. Kolliopoulos, M. Bertotti, and C. E. Banks, "Screen-printed back-to-back electroanalytical sensors: heavy metal ion sensing," Analyst, vol. 140, pp. 4130–6, 2015.

[73] A. Hayat and J. L. Marty, "Disposable screen printed electrochemical sensors: tools for environmental monitoring," Sensors (Basel), vol. 14, no. 6, pp. 10432–10453, 2014.

[74] J. Barton et al., "Screen-printed electrodes for environmental monitoring of heavy metal ions: a review," Mikrochim. Acta, vol. 183, no. 2, pp. 503–517, 2016.

[75] "CH Instruments, Inc," Chinstruments.com. [Online]. Available: https://www.chinstruments.com/. [Accessed: 05-May-2021].

[76] "Scanning electron microscopy (SEM)," Carleton.edu, 2007. [Online]. Available: https://serc.carleton.edu/research_education/geochemsheets/techniques/SEM.html. [Accessed: 07-May-2021].

[77] B. J. Inkson, "Scanning electron microscopy (SEM) and transmission electron microscopy (TEM) for materials characterization," in Materials Characterization Using Nondestructive Evaluation (NDE) Methods, G. Hübschen, I. Altpeter, R. Tschuncky, and H.-G. Herrmann, Eds. Elsevier, 2016, pp. 17–43.

[78] "Pyrrole," Chemicalbook.com. [Online]. Available: https://www.chemicalbook.com/ChemicalProductProperty_EN_CB3852794.htm. [Accessed: 12-May-2021].

[79] "Ammonium molybdate tetrahydrate," Chemicalbook.com. [Online]. Available: https://www.chemicalbook.com/ChemicalProductProperty_EN_CB3122242.htm. [Accessed: 11-May-2021].

[80] B. da S. Cerozi and K. Fitzsimmons, "The effect of pH on phosphorus availability and speciation in an aquaponics nutrient solution," *Bioresour. Technol.*, vol. 219, pp. 778–781, 2016.